A generalised structure tensor model for the mixed invariant I_8

Andrey V. Melnik*, Xiaoyu Luo, Ray W. Ogden

School of Mathematics and Statistics, University of Glasgow,

The Mathematics and Statistics Building, University of Glasgow,

University Place, Glasgow, G12 8SQ, United Kingdom

15th August 2018

Abstract

Generalised Structure Tensors (GSTs) are used to formulate constitutive models for anisotropic fibre-reinforced materials in which fibres are dispersed. The GST approach has been applied so far to models based on invariants I_4 and I_5 (I_6 and I_7). These anisotropic invariants capture the effect of deformation on each fibre family in isolation, unlike the invariant I_8, which couples two fibre families. We extend the GST approach to models based on the invariant I_8. We consider two different formulations and for each model derive expressions for stress and elasticity tensors in both the general case and for axisymmetric distributions. We apply the proposed formulation to the hyperelastic Holzapfel–Ogden model for myocardium and obtain a modified model, in which fibre dispersion is consistently accounted for in every term of the strain-energy function. We demonstrate that when accounting for fibre dispersion in the coupling term, the effect on the predicted material response can be significant and may also reduce material symmetry.

Keywords: soft tissue constitutive modelling, fibre dispersion, generalised structure tensor, deformation invariants, myocardium, anisotropic elasticity

1 Introduction

Many soft biological tissues can be regarded as elastic solid composites, consisting of an incompressible and isotropic matrix, which is reinforced by one or several families of fibres. From the perspective of constitutive modelling, the term "fibres" can be used broadly to refer to slender one-dimensional load-bearing objects. To this category belong mathematical representations for actin filaments [1], which are elements of the cytoskeleton, and for collagen and elastin [2], which are abundant in the extra-cellular matrix of connective tissues. Idealised and simplified descriptions are used for complex arrangements of fibres, which can be organised into hierarchical fibrillar units, as in tendons and ligaments [3], or into layers forming a multi-ply structure, as in the arterial wall [4]. Another example is the myocardium, in which myofibres are interconnected by fine endomysial collagen and form branching laminae, surrounded by the perimysial collagen network [5].

*Email: andrey.melnik@glasgow.ac.uk

The orientation of constituents is the central microstructural characteristic that determines the anisotropy of the tissue response. The alignment can be described via the orientation of actual fibres or in terms of a special direction that is not associated with any structural elements aligned *along* it, such as the myocardium sheet normal vector [6, 7]. Local variability of microscopic organisation is found in many tissues and can be captured at the continuum level using orientation density functions (ODFs), which express the probability of observing certain orientations within a representative volume element. This statistical datum is acquired by histological examinations using modern imaging techniques: see, e.g., [8]. For the convenience of subsequent analysis, the datum is fitted by unimodal 2D or 3D distribution functions, which reproduce the dispersion of fibres around a preferred direction, as well as the extreme cases of the strict parallel alignment and the isotropic distribution.

Structure-based constitutive models for soft tissues incorporate distributed orientation properties by means of the angular integration (AI) [9] or the generalised structure tensors (GSTs) [4, 10], which are critically compared in [11, 12] and contributions cited therein. The AI approach computes the total tissue stress as a weighted average of stresses for each possible structural orientation. The resulting expression is an integral over a range of angles, hence the name. The GST approach defines the anisotropic response using a GST, which is a weighted average of rank-one structure tensors. The GST approach has been applied to various tissues, including arteries [13, 4], myocardium [14, 15], heart valves [10], articular cartilage [16, 17], annulus fibrosus [18], and cornea [19]. The role of the GST in these models is to take into account fibre dispersion in anisotropic invariants I_4 and I_5 (I_6 and I_7), which capture the effect of deformation on each fibre family in isolation. To our knowledge, GST models for the invariant I_8 have not been considered before. This invariant couples two fibre families and is used, for instance, in models for myocardium [5] and annulus fibrosus [20].

In this paper we present a novel model for accounting for fibre dispersion in strain-energy functions that depend on the coupling invariant I_8. In Section 2 we give necessary background information and introduce notation for the GSTs. In Section 3 we consider two different formulations for the dispersed coupling invariant, discuss issues arising and derive expressions for stress and elasticity tensors in the general case and for axisymmetric distributions. In Section 4 we demonstrate the effect of accounting for fibre dispersion in the coupling invariant using a modification of the Holzapfel–Ogden model for myocardium [5]. Discussion and final remarks conclude the paper in Sections 5 and 6.

2 Invariant-based hyperelastic constitutive models

2.1 Anisotropic hyperelastic material

Consider a hyperelastic material with two distinguished directions $\mathbf{M}$ and $\mathbf{M}'$. By the representation theorem [21, 22], a general strain energy $\Psi(\mathbf{C}, \mathbf{M}, \mathbf{M}')$ can be expressed as a function of 9 invariants,

$$I_1 = \mathrm{tr}\mathbf{C} = \mathbf{1} : \mathbf{C}, \quad I_2 = \frac{1}{2}\left(\mathrm{tr}^2\mathbf{C} - \mathrm{tr}\mathbf{C}^2\right), \quad I_3 = \det\mathbf{C}, \tag{1}$$

$$I_4 = (\mathbf{M}\otimes\mathbf{M}) : \mathbf{C}, \quad I_5 = (\mathbf{M}\otimes\mathbf{M}) : \mathbf{C}^2, \tag{2}$$

$$I_6 = (\mathbf{M}'\otimes\mathbf{M}') : \mathbf{C}, \quad I_7 = (\mathbf{M}'\otimes\mathbf{M}') : \mathbf{C}^2, \tag{3}$$

$$I_8 = (\mathbf{M}\otimes\mathbf{M}') : \mathbf{C}, \quad \tilde{I}_8 = (\mathbf{M}\cdot\mathbf{M}')\mathbf{M}\cdot\mathbf{C}\mathbf{M}', \quad \hat{I}_8 = I_8^2 = (\mathbf{M}\cdot\mathbf{C}\mathbf{M}')^2 \tag{4}$$

$$I_9 = \mathbf{M}\cdot\mathbf{M}', \quad \hat{I}_9 = (\mathbf{M}\cdot\mathbf{M}')^2, \tag{5}$$

where the double contraction of two second-order tensors is defined as $\mathbf{T} : \tilde{\mathbf{T}} = \mathrm{tr}\left(\mathbf{T}\tilde{\mathbf{T}}^T\right) = \mathrm{T}_{ij}\tilde{\mathrm{T}}_{ij}$, and $\mathbf{1}$ is the identity tensor. The complete set of invariants $I_1, \dots, I_9$ is not unique, in the sense that alternative choices exist, e.g., for I_8, and I_9, which are listed above. Invariants I_9 and $\hat{I}_9$ do not depend on the deformation, their role is to define the undeformed values for $I_{8|\mathbf{C}=\mathbf{1}} = I_9$ and $\tilde{I}_{8|\mathbf{C}=\mathbf{1}} = \hat{I}_{8|\mathbf{C}=\mathbf{1}} = \hat{I}_9$. For the sake of uniformity, we define and use I_8-like invariants, whose values in the undeformed state are always zero,

$$I_{80} = I_8 - I_9 = 2\mathbf{M}\cdot\mathbf{E}\mathbf{M}', \quad \tilde{I}_{80} = \tilde{I}_8 - \hat{I}_9 = (\mathbf{M}\cdot\mathbf{M}')\left(I_8 - I_9\right), \tag{6}$$

$$\hat{I}_{80} = (I_8 - I_9)^2 = (2\mathbf{M}\cdot\mathbf{E}\mathbf{M}')^2, \tag{7}$$

where the Green–Lagrange strain tensor $\mathbf{E} = \frac{1}{2}(\mathbf{C} - \mathbf{1})$ is introduced. The use of these invariants as arguments of the strain-energy function guarantees that if the material is stress-free in the undeformed state for some choice of $\mathbf{M}$, $\mathbf{M}'$, then this is also the case for any other choice of the two vectors. Unless explicitly stated otherwise, we assume that the strain-energy function Ψ is expressed in terms I_{80}, $\tilde{I}_{80}$, or $\hat{I}_{80}$, and not in terms of I_8, $\tilde{I}_8$, or $\hat{I}_8$.

In principle, $\mathbf{M}$ and $\mathbf{M}'$ can be regarded as arbitrary directions, which are chosen for the purpose of relating material orientation—any pair of non-collinear vectors will serve this purpose. However, in fibre-reinforced materials it is convenient and customary to make no distinction between $\mathbf{M}$ and $-\mathbf{M}$ ($\mathbf{M}'$ and $-\mathbf{M}'$). In other words, the strain energy is given in the form of $\Psi(\mathbf{C}, \mathbf{M}\otimes\mathbf{M}, \mathbf{M}'\otimes\mathbf{M}')$. This identification has two consequences:

- the strain-energy function $\Psi(\mathbf{C}, \mathbf{M}\otimes\mathbf{M}, \mathbf{M}'\otimes\mathbf{M}')$ cannot depend on the sign of I_8, which is an odd functions of $\mathbf{M}$ and $\mathbf{M}'$. To ensure this, invariants $\tilde{I}_8$ or $\hat{I}_8 = I_8^2$ can be used instead of I_8. Strictly speaking, I_8 is an invariant of a function $\Psi(\mathbf{C}, \mathbf{M}, \mathbf{M}')$, but not of $\Psi(\mathbf{C}, \mathbf{M}\otimes\mathbf{M}, \mathbf{M}'\otimes\mathbf{M}')$;

- if $\mathbf{M}$ and $\mathbf{M}'$ are orthogonal, then the strain-energy functions $\Psi(\mathbf{C}, \mathbf{M}\otimes\mathbf{M}, \mathbf{M}'\otimes\mathbf{M}')$ can only describe orthotropic materials. In order to allow for general anisotropy, vectors $\mathbf{M}$ and $\mathbf{M}'$ *must not* be orthogonal. Orthotropy also arises when non-orthogonal directions $\mathbf{M}$ and $\mathbf{M}'$ are mechanically equivalent, in which case the vectors can be replaced by their bisectors, which are orthogonal, see, e.g., [23].

Thus, without loss of generality, orthotropy implies orthogonality $\mathbf{M}\cdot\mathbf{M}' = 0$. The strain energy of an orthotropic material depends, in general, only on 7 invariants, $I_1 \dots I_7$, since I_8, $\tilde{I}_8$, and $\hat{I}_8$ satisfy

$$\tilde{I}_8 = 0, \qquad I_8^2 = \hat{I}_8 = I_2 + I_5 + I_7 + I_4 I_6 - I_1(I_4 + I_6). \tag{8}$$

The second identity is given in [24] without a proof, which we provide in the Appendix A. Note that the orthogonality $\mathbf{M}\cdot\mathbf{M}' = 0$ makes I_{80} and $\hat{I}_{80}$ identical to I_8 and $\hat{I}_8$ respectively, whereas invariants $\tilde{I}_{80} = \tilde{I}_8 = 0$ become unsuitable for constitutive description.

The second Piola–Kirchhoff stress in an unconstrained hyperelastic material is given by

$$\mathbf{S} = 2\frac{\partial \Psi}{\partial \mathbf{C}} = 2\sum_i \frac{\partial \Psi}{\partial I_i}\frac{\partial I_i}{\partial \mathbf{C}}. \tag{9}$$

The stress in an incompressible material reads

$$\mathbf{S} = -p\mathbf{C}^{-1} + 2\sum_{i\neq 3} \frac{\partial \Psi}{\partial I_i}\frac{\partial I_i}{\partial \mathbf{C}}, \tag{10}$$

where p is a Lagrange multiplier corresponding to the constraint $I_3 - 1 = 0$, and any set of independent invariants can be used. The following useful identities arise from (1)–(4),

$$\frac{\partial I_1}{\partial \mathbf{C}} = \mathbf{1}, \quad \frac{\partial I_2}{\partial \mathbf{C}} = I_1\mathbf{1} - \mathbf{C}, \quad \frac{\partial I_4}{\partial \mathbf{C}} = \mathbf{M}\otimes\mathbf{M}, \quad \frac{\partial I_5}{\partial \mathbf{C}} = 2[\mathbf{C}\mathbf{M}\otimes\mathbf{M}]_{\mathrm{sym}} \tag{11}$$

$$\frac{\partial I_6}{\partial \mathbf{C}} = \mathbf{M}'\otimes\mathbf{M}', \quad \frac{\partial I_7}{\partial \mathbf{C}} = 2[\mathbf{C}\mathbf{M}'\otimes\mathbf{M}']_{\mathrm{sym}}, \quad \frac{\partial I_{80}}{\partial \mathbf{C}} = \frac{\partial I_8}{\partial \mathbf{C}} = [\mathbf{M}\otimes\mathbf{M}']_{\mathrm{sym}}, \tag{12}$$

$$\frac{\partial \tilde{I}_{80}}{\partial \mathbf{C}} = \frac{\partial \tilde{I}_8}{\partial \mathbf{C}} = (\mathbf{M}\cdot\mathbf{M}')\,[\mathbf{M}\otimes\mathbf{M}']_{\mathrm{sym}}, \quad \frac{\partial \hat{I}_{80}}{\partial \mathbf{C}} = 2I_{80}[\mathbf{M}\otimes\mathbf{M}']_{\mathrm{sym}}. \tag{13}$$

Here $[\mathbf{T}]_{\mathrm{sym}} = \frac{1}{2}\left(\mathbf{T} + \mathbf{T}^{\mathrm{T}}\right)$ denotes the symmetric part of the second order tensor $\mathbf{T}$. By using (11)–(13) in (10), we obtain

$$\mathbf{S} = -p\mathbf{C}^{-1} + 2\Psi_1\mathbf{1} + 2\Psi_2(I_1\mathbf{1} - \mathbf{C}) + 2\Psi_4\mathbf{M}\otimes\mathbf{M} + 4\Psi_5[\mathbf{C}\mathbf{M}\otimes\mathbf{M}]_{\mathrm{sym}} \tag{14}$$

$$+2\Psi_6\mathbf{M}'\otimes\mathbf{M}' + 4\Psi_7[\mathbf{C}\mathbf{M}'\otimes\mathbf{M}']_{\mathrm{sym}} + 2\Psi_{80}[\mathbf{M}\otimes\mathbf{M}']_{\mathrm{sym}}, \tag{15}$$

where $\Psi_i = \partial\Psi/\partial I_i$ with the argument omitted for brevity. If invariants $\tilde{I}_{80}$ or $\hat{I}_{80}$ are used, then the last term is replaced by either

$$2\Psi_{\tilde{8}0}\, I_9[\mathbf{M}\otimes\mathbf{M}']_{\mathrm{sym}} \quad \text{or} \quad 4\Psi_{\hat{8}0}\, I_{80}[\mathbf{M}\otimes\mathbf{M}']_{\mathrm{sym}}, \tag{16}$$

where Ψ_{80}, $\Psi_{\tilde{8}0}$, and $\Psi_{\hat{8}0}$ denote partial derivatives with respect to I_{80}, $\tilde{I}_{80}$, and $\hat{I}_{80}$, respectively.

2.2 The GST model

Consider a family of distributed (dispersed) fibres, whose orientation is given by an even orientation density function (ODF) $\rho(\mathbf{N})=\rho(-\mathbf{N})$. The original GST model [4] accounts for the distributed fibre reinforcement and extends a material model based on a fibre potential $\psi_{\mathrm{f}}(I_4)$ as follows,

$$\Psi_{\mathrm{GST}} = \psi_{\mathrm{f}}(I_4^*) = \psi_{\mathrm{f}}(\mathbf{H}:\mathbf{C}), \qquad \mathbf{H} = \int_{\mathbb{S}^2} \rho(\mathbf{N})\mathbf{N}\otimes\mathbf{N}d\omega, \tag{17}$$

where $\mathbf{H}$ is the generalised structure tensor (GST), $\mathbb{S}^2 = \{\mathbf{N}\in\mathbb{R}^3, |\mathbf{N}| = 1\}$ denotes the unit sphere, $\mathbf{N}$ is the direction of integration, $d\omega$ is the solid angle element in the direction $\mathbf{N}$. We use $\oint_{\mathbb{S}^2} \rho d\omega = 1$ as the normalisation condition for ρ. An alternative condition $\oint_{\mathbb{S}^2} \rho d\omega = 4\pi$ is used by other authors.

The unit vector $\mathbf{N}$ denotes one of many possible fibre directions and is distinguished from $\mathbf{M}$, which appears in (2) and denotes there a predetermined direction of anisotropy. One may as well regard $\mathbf{N}$ as a stochastic analogue of the deterministic vector $\mathbf{M}$, that is, $I_4(\mathbf{N})$ is the analogue to

$I_4(\mathbf{M})$, etc. The modified invariant I_4^* can be regarded as the average of $I_4(\mathbf{N})$ weighted by $\rho(\mathbf{N})$. Hence, the argument of the fibre potential $\psi_\mathrm{f}(I_4)$ is replaced by its average:

$$I_4(\mathbf{N}) = (\mathbf{N}\otimes\mathbf{N}) : \mathbf{C} \quad \rightarrow \quad I_4^\star = \mathbf{H} : \mathbf{C}. \tag{18}$$

Phenomenological constitutive parameters must be fitted to experimental data using the modified fibre potential $\psi_\mathrm{f}(I_4^*)$ and not the original function $\psi_\mathrm{f}(I_4)$. Doing so is important to ensure that the descriptive and predictive capabilities of the GST model are fully used [11].

2.2.1 Extension of the GST approach to multiple fibre families and invariant I_5

The same procedure, as above, can be applied to a material containing several families, if the strain energy of each of them depends on an I_4-like invariant,

$$\sum_{i=1}^{n} \psi_\mathrm{f}^{(i)}(I_{4,i}) \quad \rightarrow \quad \sum_{i=1}^{n} \psi_\mathrm{f}^{(i)}(I_{4,i}^\star), \qquad I_{4,i}^\star = \mathbf{H}^{(i)} : \mathbf{C}, \tag{19}$$

where, in general, $\psi_\mathrm{f}^{(i)}(I_{4,i}^\star)$ are n different functions, and $\mathbf{H}^{(i)}$ are based on n different distributions $\rho^{(i)}(\mathbf{N}^{(i)})$. In particular, we can replace I_4 and I_6 for $I_4^\star = \mathbf{H} : \mathbf{C}$ and $I_6^\star = \mathbf{H}' : \mathbf{C}$, where $\mathbf{H}$ and $\mathbf{H}'$ are GSTs computed based on ODFs $\rho(\mathbf{N})$ and $\rho'(\mathbf{N}')$ respectively. See Figure 1 for a schematic representation of a material with two fibre families.

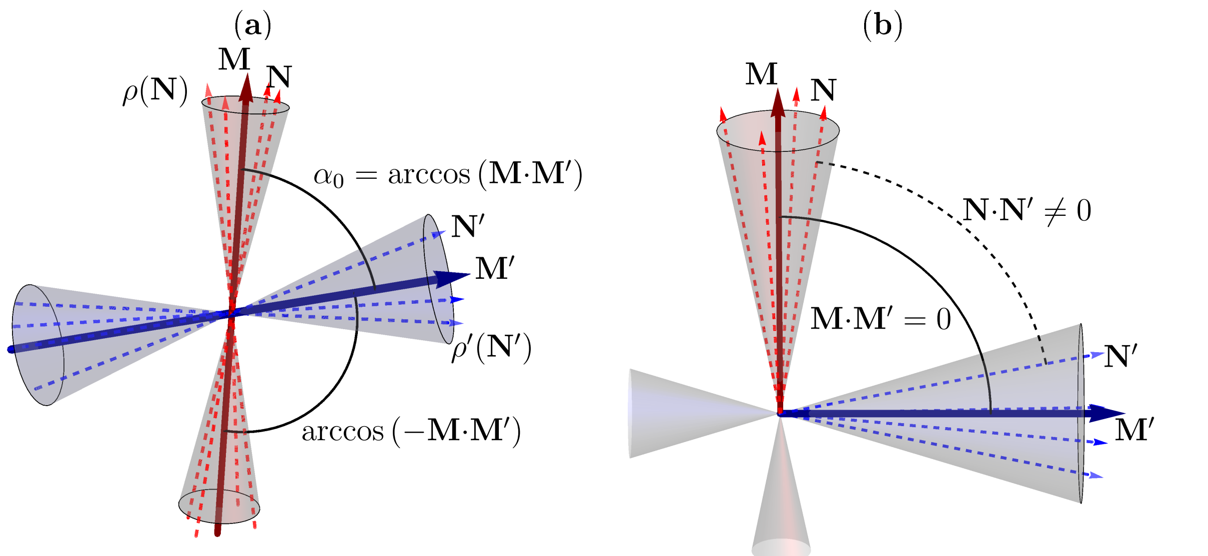

Figure 1: Two families of dispersed fibres with mean directions $\mathbf{M}$ and $\mathbf{M}'$. Vectors $\mathbf{N}$ and $\mathbf{N}'$ correspond to one of many possible fibre orientations in the respective fibre families, and are the variables of integration in the computation of an average weighted by orientation density functions $\rho(\mathbf{N})$ and $\rho'(\mathbf{N}')$. (a) Non-orthogonal mean fibre directions with angle $\alpha_0 = \arccos \mathbf{M} \cdot \mathbf{M}' \neq \frac{\pi}{2}$. Even though the material structure is invariant with respect to inverting the direction of $\mathbf{M}$ or $\mathbf{M}'$, the sign of $\cos\alpha_0 = \mathbf{M}\cdot\mathbf{M}'$ will change. (b) In the case of orthogonal mean fibre directions ($\mathbf{M}\cdot\mathbf{M}' = 0$) particular fibre directions within a dispersion are not necessarily orthogonal ($\mathbf{N}\cdot\mathbf{N}' \neq 0$).

Holzapfel and Ogden [11] provide an analogous expression for the modification of invariant I_5,

$$I_5(\mathbf{N}) = (\mathbf{N}\otimes\mathbf{N}) : \mathbf{C}^2 \rightarrow I_5^\star = \mathbf{H} : \mathbf{C}^2. \tag{20}$$

Similarly, we can define $I_7^\star = \mathbf{H}' : \mathbf{C}^2$ for the second fibre family, and $I_{5,i}^\star = \mathbf{H}^{(i)} : \mathbf{C}^2$ for the ith fibre family.

2.2.2 Axisymmetric fibre distribution

When the fibre distribution is assumed to be axisymmetric with respect to some direction $\mathbf{M}$ (which is called the mean fibre direction), i.e. $\rho(\mathbf{N}) = \tilde{\rho}(\theta) = \tilde{\rho}(\arccos \mathbf{N}\cdot\mathbf{M})$, the GST takes a particularly simple form,

$$\mathbf{H} = \kappa\mathbf{1} + (1-3\kappa)\mathbf{M}\otimes\mathbf{M}, \qquad \kappa = \pi\int_0^\pi \tilde{\rho}(\theta)\sin^3\theta d\theta. \tag{21}$$

The corresponding model is called *"kappa-model"* [4, 13], as the GST $\mathbf{H}$ captures the extent of orientational dispersion using a single scalar, the dispersion parameter κ. The modified invariants are given by

$$I_4^* \equiv \mathbf{H}:\mathbf{C} = \kappa I_1 + (1-3\kappa)I_4, \qquad I_5^* \equiv \mathbf{H}:\mathbf{C}^2 = \kappa(I_1^2 - 2I_2) + (1-3\kappa)I_5, \tag{22}$$

where I_4 and I_5 are the standard anisotropic invariants corresponding to the mean fibre direction $\mathbf{M}$. Here we used identities (2) and $\mathbf{1}:\mathbf{C}^2 = I_1^2 - 2I_2$, which follows from (1).

2.2.3 Extension of the GST approach to I_8

To our knowledge, no modification similar to (18) and (20) was previously considered for I_8. Such modification can be used to model fibre splay or orientation uncertainty in materials with two fibre families, whose strain energy has a term of the form $\psi(I_8)$ or similar. An example of such material is the myocardium, wherein two material directions, labelled $\mathbf{f}$ and $\mathbf{s}$, are distinguished. Although GST models for distributed (dispersed) directions in myocardium have recently been proposed [14, 15], these studies used constitutive models with the regular invariant $I_{8\text{fs}}$ and the modified invariants $I_\text{f}^\star$, $I_\text{s}^\star$. In other words, the models did not consider the effect of directional dispersion on the mixed term $\psi_\text{fs}(I_{8\text{fs}})$.

In this contribution, we consider a GST-based modification procedure for I_{80}, $\tilde{I}_{80}$, and $\hat{I}_{80}$, thereby extend the GST approach to a complete set of anisotropic invariants. The proposed full GST model defines the second Piola–Kirchhoff stress tensor for a general incompressible material with two dispersed orientations by

$$\begin{aligned} \mathbf{S} \;=\; & -p\mathbf{C}^{-1} + 2\Psi_1\mathbf{1} + 2\Psi_2(I_1\mathbf{1} - \mathbf{C}) + 2\Psi_4\mathbf{H} + 4\Psi_5[\mathbf{CH}]_\text{sym} & (23)\\ & +2\Psi_6\mathbf{H}' + 4\Psi_7[\mathbf{CH}']_\text{sym} + 4\Psi_{\hat{8}0}\,[\mathbf{H}\,(\mathbf{C}-\mathbf{1})\,\mathbf{H}']_\text{sym}\,, & (24) \end{aligned}$$

or, alternatively, by the same expression with the last term replaced by

$$2\Psi_{\tilde{8}0}\,[\mathbf{HH}']_\text{sym}, \tag{25}$$

where modified anisotropic invariants are used throughout, i.e. $\Psi_i = \partial\Psi/\partial I_i^\star$, $i = 4,\ldots,7,80$. The original expressions without dispersion (14)–(16) can be recovered from the GST model by replacing the GSTs $\mathbf{H}$, $\mathbf{H}'$ in (23)–(25) with the rank-one structure tensors $\mathbf{M}\otimes\mathbf{M}$, $\mathbf{M}'\otimes\mathbf{M}'$. The Cauchy stress tensor is defined as the push forward of the second Piola–Kirchhoff stress tensor,

$$\begin{aligned} \boldsymbol{\sigma} = \mathbf{FSF}^T = & -p\mathbf{1} + 2\Psi_1\mathbf{b} + 2\Psi_2(I_1\mathbf{b} - \mathbf{b}^2) + 2\Psi_4\mathbf{h} + 4\Psi_5[\mathbf{bh}]_\text{sym} & (26)\\ & + 2\Psi_6\mathbf{h}' + 4\Psi_7[\mathbf{bh}']_\text{sym} + 4\Psi_{\hat{8}0}\,\left[\mathbf{h}\left(\mathbf{1}-\mathbf{b}^{-1}\right)\mathbf{h}'\right]_\text{sym}\,, & (27) \end{aligned}$$

where $\mathbf{h} = \mathbf{F}\mathbf{H}\mathbf{F}^T$, $\mathbf{h} = \mathbf{F}'\mathbf{H}'\mathbf{F}^T$ are the structure tensors pushed forward into the current configuration and $\mathbf{b} = \mathbf{F}\mathbf{F}^T$ is the left Cauchy–Green deformation tensor.

In the remainder of this paper, we derive the GST model for modified invariants $\tilde{I}_{80}^\star$, $\hat{I}_{80}^\star$, explain why invariants $I_8^\star$ or $I_{80}^\star$ cannot be used, and illustrate the effect of dispersion in the mixed term using an orthotropic model for the myocardium.

3 Modified invariants $I_{80}^\star$, $\tilde{I}_{80}^\star$, and $\hat{I}_{80}^\star$

We introduce the following notation,

$$\langle\bullet\rangle \equiv \int_{\mathbb{S}^2} \bullet\rho(\mathbf{N})d\omega, \quad \langle\bullet\rangle' \equiv \int_{\mathbb{S}^2} \bullet\rho'(\mathbf{N}')d\omega, \tag{28}$$

where $\langle\bullet\rangle$ and $\langle\bullet\rangle'$ are the (weighted) averaging operators, as they are linear, idempotent and normalised in the sense that $\langle 1\rangle = \langle 1\rangle' = 1$. The modified invariants I_i^* can be regarded as the averaged counterparts of the original invariants I_i, and the GSTs are thought of as the averaged rank-one symmetric structure tensors,

$$I_4^\star = \langle I_4(\mathbf{N})\rangle = \langle(\mathbf{N}\otimes\mathbf{N}){:}\mathbf{C}\rangle = \mathbf{H}{:}\mathbf{C}, \qquad I_5^\star = \langle I_5(\mathbf{N})\rangle = \langle(\mathbf{N}\otimes\mathbf{N}){:}\mathbf{C}^2\rangle = \mathbf{H}{:}\mathbf{C}^2, \tag{29}$$

$$I_6^\star = \langle I_6(\mathbf{N}')\rangle' = \langle(\mathbf{N}'\otimes\mathbf{N}'){:}\mathbf{C}\rangle' = \mathbf{H}'{:}\mathbf{C}, \quad I_7^\star = \langle I_7(\mathbf{N}')\rangle' = \langle(\mathbf{N}'\otimes\mathbf{N}'){:}\mathbf{C}^2\rangle' = \mathbf{H}'{:}\mathbf{C}^2. \tag{30}$$

In a similar way, we consider the weighted average of I_{80} with respect to orientation distributions of $\mathbf{N}$ and $\mathbf{N}'$, since I_{80} depends on both directions. We define

$$I_{80}^\star = \langle\langle I_{80}(\mathbf{N},\mathbf{N}')\rangle\rangle' = 2\langle\langle \mathbf{N}\cdot\mathbf{E}\mathbf{N}'\rangle\rangle'. \tag{31}$$

Note that I_{80} is an odd function of $\mathbf{N}$ and $\mathbf{N}'$. Therefore, its average over the entire unit sphere with respect to even orientation functions $\rho(\mathbf{N})$ and $\rho'(\mathbf{N}')$ is identically zero,

$$I_{80}^\star = \langle\langle I_{80}(\mathbf{N},\mathbf{N}')\rangle\rangle' \equiv 0. \tag{32}$$

Obviously, a definition of a strain-energy function with a constant argument $I_8^\star \equiv 0$ or $I_{80}^\star \equiv 0$ is of no use. Therefore, we investigate models based on the averaging of invariants $\tilde{I}_{80}$ and $\hat{I}_{80}$, which are even functions of the special directions.

3.1 Invariants $\tilde{I}_{80}$ and $\tilde{I}_{80}^*$

The average of $\tilde{I}_{80}$ is defined as

$$\tilde{I}_{80}^\star = \langle\langle \tilde{I}_{80}(\mathbf{N},\mathbf{N}')\rangle\rangle' = 2\langle\langle(\mathbf{N}\cdot\mathbf{N}')\,\mathbf{N}\cdot\mathbf{E}\mathbf{N}'\rangle\rangle'. \tag{33}$$

In order to express it via the GST, we write

$$\begin{aligned}\tilde{I}_{80}^\star &= 2\langle\langle(\mathbf{N}\otimes\mathbf{N})(\mathbf{N}'\otimes\mathbf{N}') : \mathbf{E}\rangle\rangle' = 2\langle\mathbf{N}\otimes\mathbf{N}\rangle\langle\mathbf{N}'\otimes\mathbf{N}'\rangle' : \mathbf{E} \\ &= 2(\mathbf{H}\mathbf{H}') : \mathbf{E} = 2[\mathbf{H}\mathbf{H}']_{\text{sym}} : \mathbf{E},\end{aligned} \tag{34}$$

where we have used the fact that the integrand can separated into factors depending respectively on $\mathbf{N}$, $\mathbf{N}'$, and $\mathbf{E}$. Hence, we can define a structure-like tensor

$$\tilde{\mathbf{H}} = [\mathbf{H}\mathbf{H}']_{\text{sym}}, \quad \text{so that} \quad \tilde{I}_{80}^\star = 2\tilde{\mathbf{H}} : \mathbf{E}. \tag{35}$$

Remark 1. The second-order structure-like tensor $\tilde{\mathbf{H}}$ is symmetric, but unlike the generalised structure tensor, it is not necessarily positive semi-definite. For illustration, consider the strict fibre alignment case, and the following eigendecomposition,

$$\tilde{\mathbf{H}} \;=\; \frac{1}{2}(\mathbf{M}\cdot\mathbf{M}')\,(\mathbf{M}\otimes\mathbf{M}'+\mathbf{M}'\otimes\mathbf{M}) = \tilde{\lambda}_1\tilde{\mathbf{E}}_1\otimes\tilde{\mathbf{E}}_1+\tilde{\lambda}_2\tilde{\mathbf{E}}_2\otimes\tilde{\mathbf{E}}_2, \tag{36}$$

where $\tilde{\lambda}_{1,2}=\frac{1}{2}(\mathbf{M}\cdot\mathbf{M}')(\mathbf{M}\cdot\mathbf{M}'\pm 1)$, $\quad \tilde{\mathbf{E}}_{1,2}=(\mathbf{M}\pm\mathbf{M}')|\mathbf{M}\pm\mathbf{M}'|^{-1}$, and the eigenvalues $\tilde{\lambda}_{1,2}$ of $\tilde{\mathbf{H}}$ are clearly of opposite sign. The lack of positive semi-definiteness is related to the fact that $\tilde{I}^{\star}_{80}$ can take arbitrary large in magnitude positive and negative values, as for $\mathbf{E}=\alpha(\mathbf{M}\pm\mathbf{M}')\otimes(\mathbf{M}\pm\mathbf{M}')$ we get $\tilde{I}^{\star}_{80}=\alpha(\mathbf{M}\cdot\mathbf{M}')(\mathbf{M}\cdot\mathbf{M}'\pm 1)^2$, and such deformations are feasible in the sense that $\mathbf{F}=\mathbf{U}=(2\mathbf{E}+\mathbf{1})^{1/2}$ is a well-defined deformation gradient, which satisfies $\det\mathbf{F}>0$. The absence of the infimum makes invariants $\tilde{I}_{80}$ and $\tilde{I}_8$ less attractive for formulation of elastic potentials than the quadratic invariant $\hat{I}_{80}$. See [25] for a review of hyperelastic strain energies.

One can also define

$$\tilde{I}^{\star}_8=\langle\langle\tilde{I}_8(\mathbf{N},\mathbf{N}')\rangle\rangle'=\langle\langle(\mathbf{N}\cdot\mathbf{N}')\,\mathbf{N}\cdot\mathbf{C}\mathbf{N}'\rangle\rangle'=[\mathbf{H}\mathbf{H}']_{\text{sym}}:\mathbf{C}=\tilde{\mathbf{H}}:\mathbf{C}, \tag{37}$$

and establish the relation between $\tilde{I}^{\star}_8$ and $\tilde{I}^{\star}_{80}$,

$$\tilde{I}^{\star}_{80}=\langle\langle I_9(\mathbf{N},\mathbf{N}')I_8(\mathbf{N},\mathbf{N}')-(I_9(\mathbf{N},\mathbf{N}'))^2\rangle\rangle'=\tilde{I}^{\star}_8-\tilde{I}^{\star}_9=\tilde{\mathbf{H}}:\mathbf{C}-\mathrm{tr}\tilde{\mathbf{H}}. \tag{38}$$

The derivatives of $\tilde{I}^{\star}_{80}$ and $\tilde{I}^{\star}_8$ are given by

$$\frac{\partial\tilde{I}^{\star}_8}{\partial\mathbf{C}}=\frac{\partial\tilde{I}^{\star}_{80}}{\partial\mathbf{C}}=\tilde{\mathbf{H}},\qquad \frac{\partial^2\tilde{I}^{\star}_{80}}{\partial\mathbf{C}\partial\mathbf{C}}=\frac{\partial^2\tilde{I}^{\star}_8}{\partial\mathbf{C}\partial\mathbf{C}}=\mathbb{0} \tag{39}$$

The second Piola–Kirchhoff stress contribution due to the fibre potentials $\tilde{\psi}(\tilde{I}^{\star}_{80})$ and $\tilde{\psi}(\tilde{I}^{\star}_8)$ have the identical form,

$$2\frac{\partial}{\partial\mathbf{C}}\tilde{\psi}(\tilde{I}^{\star}_{80})=2\frac{\partial\tilde{\psi}}{\partial\tilde{I}^{\star}_{80}}\frac{\partial\tilde{I}^{\star}_{80}}{\partial\mathbf{C}}=2\tilde{\psi}'_{\tilde{8}}\,\tilde{\mathbf{H}}. \tag{40}$$

The same applies to the Lagrangian elasticity tensor contribution due to $\tilde{\psi}(\tilde{I}^{\star}_{80})$ and $\tilde{\psi}(\tilde{I}^{\star}_8)$, which read

$$4\frac{\partial^2}{\partial\mathbf{C}\partial\mathbf{C}}\tilde{\psi}(\tilde{I}^{\star}_{80})=4\frac{\partial^2}{\partial\mathbf{C}\partial\mathbf{C}}\tilde{\psi}(\tilde{I}^{\star}_8)=4\left(\frac{\partial^2\tilde{\psi}}{\partial\tilde{I}^{\star}_{80}\partial\tilde{I}^{\star}_{80}}\frac{\partial\tilde{I}^{\star}_{80}}{\partial\mathbf{C}}\otimes\frac{\partial\tilde{I}^{\star}_{80}}{\partial\mathbf{C}}+\frac{\partial\tilde{\psi}}{\partial\tilde{I}^{\star}_8}\frac{\partial^2\tilde{I}^{\star}_{80}}{\partial\mathbf{C}\partial\mathbf{C}}\right)=4\tilde{\psi}''_{\tilde{8}}\,\tilde{\mathbf{H}}\otimes\tilde{\mathbf{H}}. \tag{41}$$

Axisymmetric distributions

In the case of axisymmetric fibre distributions, the GSTs have the special form

$$\mathbf{H}=\kappa\mathbf{1}+(1-3\kappa)\mathbf{A},\qquad \mathbf{H}'=\kappa'\mathbf{1}+(1-3\kappa')\mathbf{A}', \tag{42}$$

where $\mathbf{A}=\mathbf{M}\otimes\mathbf{M}$, $\mathbf{A}'=\mathbf{M}'\otimes\mathbf{M}'$. The second-order structure-like tensor reads

$$\tilde{\mathbf{H}}=[\mathbf{H}\mathbf{H}']_{\text{sym}}=\kappa\kappa'\mathbf{1}+\kappa'(1-3\kappa)\mathbf{A}+\kappa(1-3\kappa')\mathbf{A}'+(1-3\kappa)(1-3\kappa')[\mathbf{A}\mathbf{A}']_{\text{sym}}. \tag{43}$$

Double contractions $\tilde{\mathbf{H}} : \mathbf{C}$ and $2\tilde{\mathbf{H}} : \mathbf{E}$ yield, respectively,

$$\begin{aligned}\tilde{I}_8^\star &= \kappa\kappa' I_1 + \kappa'(1-3\kappa) I_4 + \kappa(1-3\kappa') I_6 + (1-3\kappa)(1-3\kappa')\tilde{I}_8, &(44)\\ \tilde{I}_{80}^\star &= \kappa\kappa'\,(I_1-3) + \kappa'(1-3\kappa)\,(I_4-1) + \kappa(1-3\kappa')\,(I_6-1) + (1-3\kappa)(1-3\kappa')\tilde{I}_{80}, &(45)\end{aligned}$$

since $I_1 = \mathbf{1} : \mathbf{C}$, $I_4 = \mathbf{A} : \mathbf{C}$, $I_6 = \mathbf{A}' : \mathbf{C}$, $\tilde{I}_8 = \mathbf{A}\mathbf{A}' : \mathbf{C}$.

As expected, $\kappa = \kappa' = 0$ recovers the strict alignment case, $\tilde{I}_{80}^\star = \tilde{I}_{80}$ and $\tilde{I}_8^\star = \tilde{I}_8$. The fully isotropic case $\kappa = \kappa' = \frac{1}{3}$ yields $\tilde{I}_{80}^\star = \frac{1}{9}(I_1 - 3)$, $\tilde{I}_8^\star = \frac{1}{9} I_1$. When one family is isotropic ($\kappa' = \frac{1}{3}$), invariants $\tilde{I}_8^\star$ and $\tilde{I}_{80}^\star$ capture the average squares of stretch and strain of the other family, $\tilde{I}_{80}^\star = \frac{1}{3}(\tilde{I}_4^\star - 1)$, $\tilde{I}_8^\star = \frac{1}{3}\tilde{I}_4^\star$. In a particular case of orthogonal alignment of families, $(\mathbf{M}\cdot\mathbf{M}')^2 = \mathbf{A} : \mathbf{A}' = 0$, the last term in (44) disappears, as $\tilde{I}_{80} = 0$ identically.

The contribution to the second Piola–Kirchhoff stress for the axisymmetric case reads

$$2\frac{\partial}{\partial \mathbf{C}}\tilde{\psi}(\tilde{I}_{80}^\star) = 2\tilde{\psi}_{\bar{8}}'\,\left(\kappa\kappa'\mathbf{1} + \kappa'(1-3\kappa)\mathbf{A} + \kappa(1-3\kappa')\mathbf{A}' + (1-3\kappa)(1-3\kappa')[\mathbf{A}\mathbf{A}']_{\mathrm{sym}}\right). \tag{46}$$

The special form of the elasticity tensor contribution can be computed by using (43) in (41).

3.2 Invariants $\hat{I}_8$ and $\hat{I}_8^*$

The average of $\hat{I}_{80}$ is defined as

$$\hat{I}_{80}^\star = \langle\langle \hat{I}_{80}(\mathbf{N}, \mathbf{N}')\rangle\rangle' = 2\langle\langle (\mathbf{N}\cdot\mathbf{E}\mathbf{N}')^2\rangle\rangle'. \tag{47}$$

It follows that

$$\begin{aligned}\hat{I}_{80}^\star &= 2\langle\langle (\mathbf{N}\cdot\mathbf{E}\mathbf{N}')^2\rangle\rangle' = 4\langle\langle \mathbf{N}\otimes\mathbf{N}'\otimes\mathbf{N}\otimes\mathbf{N}'\rangle\rangle' :: \mathbf{E}\otimes\mathbf{E}\\ &= 4(\mathbf{H}\bar{\otimes}\mathbf{H}') :: \mathbf{E}\otimes\mathbf{E} = 4[\mathbf{H}\bar{\otimes}\mathbf{H}']_{\mathrm{sym}} :: \mathbf{E}\otimes\mathbf{E} &(48)\end{aligned}$$

where again we relied on the fact that the integrand can be separated into factors depending respectively on $\mathbf{N}$, $\mathbf{N}'$, and $\mathbf{E}$. We introduce the quadruple contraction of two fourth-order tensors, defined as $\mathbb{T} :: \tilde{\mathbb{T}} = \mathbb{T}_{ijkl}\tilde{\mathbb{T}}_{ijkl}$, and the modified tensor products $\bar{\otimes}$ and $\underline{\otimes}$, defined as $[\mathbf{A}\bar{\otimes}\mathbf{B}]_{ijkl} = \mathrm{A}_{ik}\mathrm{B}_{jl}$, $[\mathbf{A}\underline{\otimes}\mathbf{B}]_{ijkl} = \mathrm{A}_{il}\mathrm{B}_{kj}$. The fourth-order tensor $\mathbf{E}\otimes\mathbf{E}$ possess both major and minor symmetries, whereas $[\mathbf{H}\bar{\otimes}\mathbf{H}']_{ijkl} = \mathrm{H}_{ik}\mathrm{H}'_{jl}$ has only the major symmetry (a fourth-order tensor C is said to have major or minor symmetries if, respectively, $\mathsf{C}_{ijkl} = \mathsf{C}_{klij}$ or $\mathsf{C}_{ijkl} = \mathsf{C}_{ijlk} = \mathsf{C}_{jikl}$). Nevertheless, the minor symmetries can be imposed upon $\mathbf{H}\bar{\otimes}\mathbf{H}'$ for the purpose of computing $\hat{I}_{80}^\star$ and its derivatives. Thus, we can define the fourth-order structure tensor as

$$\hat{\mathbb{H}} = [\mathbf{H}\bar{\otimes}\mathbf{H}']_{\mathrm{sym}} = \frac{1}{4}(\mathbf{H}\bar{\otimes}\mathbf{H}' + \mathbf{H}'\bar{\otimes}\mathbf{H} + \mathbf{H}\underline{\otimes}\mathbf{H}' + \mathbf{H}'\underline{\otimes}\mathbf{H}), \quad \text{so that} \quad \hat{I}_{80}^\star = 4\hat{\mathbb{H}} :: \mathbf{E}\otimes\mathbf{E}. \tag{49}$$

The fourth-order and second-order structure-like tensors are related via $\tilde{\mathbf{H}} = \hat{\mathbb{H}} : \mathbf{1} = \mathbf{1} : \hat{\mathbb{H}}$.

One can also define

$$\hat{I}_8^\star = \langle\langle (I_8(\mathbf{N}, \mathbf{N}'))^2\rangle\rangle' = \langle\langle (\mathbf{N}\cdot\mathbf{C}\mathbf{N}')^2\rangle\rangle' = \hat{\mathbb{H}} :: \mathbf{C}\otimes\mathbf{C}, \tag{50}$$

and establish the relation

$$\hat{I}_{80}^\star = \hat{I}_8^\star - 2\tilde{I}_8^\star + \hat{I}_9^\star = \hat{I}_8^\star - 2\tilde{I}_{80}^\star - \hat{I}_9^\star, \tag{51}$$

where $\tilde{I}_{80}^*$, $\tilde{I}_8^*$ are defined in (35), (37), and $\hat{I}_9^\star = \hat{I}^\star_{8|\mathbf{C}=\mathbf{1}} = \hat{\mathbb{H}} :: \mathbf{1}\otimes\mathbf{1} = \mathrm{tr}\tilde{\mathbf{H}}$.

Remark 2. In general, $\mathbf{C}\otimes\mathbf{C}$ and $\hat{\mathbb{H}} = [\mathbf{H}\bar{\otimes}\mathbf{H}']_{\mathrm{sym}}$ possess major and minor symmetries, but are not invariant with respect to any permutation of dimensions, e.g., $[\mathbf{H}\bar{\otimes}\mathbf{H}']_{\mathrm{sym}} \neq \frac{1}{2}\left(\mathbf{H}\otimes\mathbf{H}' + \mathbf{H}'\otimes\mathbf{H}\right)$. If this were the case, then one could use the spectral representation $\hat{\mathbb{H}} = \sum_{i=1}^{3} \hat{h}_i \hat{\mathbf{E}}_i\otimes\hat{\mathbf{E}}_i\otimes\hat{\mathbf{E}}_i\otimes\hat{\mathbf{E}}_i$ for a general material structure, while in fact it holds only for some special cases (e.g., when $\mathbf{H}$ and $\mathbf{H}'$ are coaxial). If $\hat{\mathbb{H}}$ is regarded as a bilinear operator acting in the linear space of second-order tensors, then it is symmetric (major symmetries) and positive semi-definite. The latter follows from $4\mathbf{E} : \hat{\mathbb{H}} : \mathbf{E} = \hat{I}_{80}^{\star} \geq 0$, where $\mathbf{E}$ is an arbitrary second-order tensor. This holds by virtue of (48) and does not require $\mathbf{E}$ to be the Green–Lagrange strain tensor, although its symmetric part is proportional to some Green–Lagrange strain tensor.

The derivatives of $\hat{I}_{80}^{\star}$ are given by

$$\frac{\partial \hat{I}_{80}^{\star}}{\partial \mathbf{C}} = 2\hat{\mathbb{H}} : 2\mathbf{E} = 2\left[\mathbf{H}\left(\mathbf{C} - \mathbf{1}\right)\mathbf{H}'\right]_{\mathrm{sym}}, \qquad \frac{\partial \hat{I}_{8}^{\star}}{\partial \mathbf{C}} = 2\hat{\mathbb{H}} : \mathbf{C} = \frac{\partial \hat{I}_{80}^{\star}}{\partial \mathbf{C}} + 2\tilde{\mathbf{H}}, \tag{52}$$

$$\frac{\partial^2 \hat{I}_{80}^{\star}}{\partial \mathbf{C}\partial \mathbf{C}} = \frac{\partial^2 \hat{I}_{8}^{\star}}{\partial \mathbf{C}\partial \mathbf{C}} = 2\hat{\mathbb{H}} = 2[\mathbf{H}\bar{\otimes}\mathbf{H}']_{\mathrm{sym}}. \tag{53}$$

The second Piola–Kirchhoff stress contribution due to the fibre potential $\hat{\psi}(\hat{I}_{80}^{\star})$ is given by

$$2\frac{\partial}{\partial \mathbf{C}}\hat{\psi}(\hat{I}_{80}^{\star}) = 4\frac{\partial \hat{\psi}}{\hat{I}_{80}^{\star}}\left[\mathbf{H}\left(\mathbf{C} - \mathbf{1}\right)\mathbf{H}'\right]_{\mathrm{sym}} = 8\hat{\psi}'_{\hat{8}0}\,\hat{\mathbb{H}} : \mathbf{E}. \tag{54}$$

The corresponding contribution to the Lagrangian elasticity tensor reads

$$4\frac{\partial^2}{\partial \mathbf{C}\partial \mathbf{C}}\hat{\psi}(\hat{I}_{80}^{\star}) = 4\left(\frac{\partial^2 \hat{\psi}}{\partial \hat{I}_{80}^{\star}\partial \hat{I}_{80}^{\star}}\frac{\partial \hat{I}_{80}^{\star}}{\partial \mathbf{C}}\otimes\frac{\partial \hat{I}_{80}^{\star}}{\partial \mathbf{C}} + \frac{\partial \hat{\psi}}{\partial \hat{I}_{80}^{\star}}\frac{\partial^2 \hat{I}_{80}^{\star}}{\partial \mathbf{C}\partial \mathbf{C}}\right) \tag{55}$$

$$= 64\hat{\psi}''_{\hat{8}0}\left(\hat{\mathbb{H}} : \mathbf{E}\right)\otimes\left(\hat{\mathbb{H}} : \mathbf{E}\right) + 8\hat{\psi}'_{\hat{8}0}\,\hat{\mathbb{H}} \tag{56}$$

Next, we specialise the above expressions for the case of axisymmetric distributions. Similar expressions for the case of non-axisymmetrically distributed but coaxially aligned fibre families are included in Appendix B.

Remark 3. The choice of invariants $\tilde{I}_{80}$ and $\hat{I}_{80}$ is motivated by the possibility of using the same strain-energy function for different material structures. To predict a stress-free state in the undeformed configuration, the strain-energy function must satisfy $\frac{\partial}{\partial \mathbf{C}}\psi = \mathbf{0}$ at $\mathbf{C} = \mathbf{1}$, for which $\tilde{I}_8 = \hat{I}_8 = \hat{I}_9 = (\mathbf{M}\cdot\mathbf{M}')^2$. Therefore, a particular form of the strain-energy function has to be adjusted to a considered material structure. As for the averaged invariants $\tilde{I}_8^{\star}$, $\hat{I}_8^{\star}$, the undeformed values can be taken into account for the whole structure, $\hat{I}_9^{\star}$, or for each combination of test direction, $\hat{I}_9(\mathbf{N},\mathbf{N}')$. These two options applied to $\hat{I}_8 = I_8^2$ correspond to the functional dependence on $\langle\langle I_8^2 - I_9^2\rangle\rangle'$ and $\langle\langle (I_8 - I_9)^2\rangle\rangle'$. The latter option is chosen, because it guarantees positiveness for the full range of deformation. When applied to $\tilde{I}_8 = I_9 I_8$, the two options are equivalent.

Axisymmetric distributions case

When the ODFs ρ and ρ' are both axisymmetric, the second-order GSTs are given by (42), and the fourth-order structure tensor reads

$$\mathbb{H} = \kappa\kappa'\mathbf{1}\bar{\otimes}\mathbf{1} + \kappa'(1-3\kappa)[\mathbf{A}\bar{\otimes}\mathbf{1}]_{\mathrm{sym}} + \kappa(1-3\kappa')[\mathbf{1}\bar{\otimes}\mathbf{A}']_{\mathrm{sym}} + (1-3\kappa)(1-3\kappa')[\mathbf{A}\bar{\otimes}\mathbf{A}']_{\mathrm{sym}}, \tag{57}$$

wherein $[[\mathbf{A}\bar{\otimes}\mathbf{A}']_{\text{sym}}]_{ijkl} = \frac{1}{4}\left(\mathrm{A}_{ik}\mathrm{A}'_{jl} + \mathrm{A}_{jk}\mathrm{A}'_{il} + \mathrm{A}_{il}\mathrm{A}'_{jk} + \mathrm{A}_{jl}\mathrm{A}'_{ik}\right)$ etc.

In this special case, the derivative $\partial\hat{I}^{\star}_{80}/\partial\mathbf{C}$ is evaluated using (57), (52). The stress contribution reads

$$2\frac{\partial}{\partial\mathbf{C}}\hat{\psi}(\hat{I}^{\star}_{80}) = 2\frac{\partial\hat{\psi}}{\partial\hat{I}^{\star}_{80}}\frac{\partial\hat{I}^{\star}_{80}}{\partial\mathbf{C}} = 4\hat{\psi}'_{\hat{8}0}\Big(\kappa\kappa'2\mathbf{E} + \kappa'(1-3\kappa)[2\mathbf{E}\mathbf{A}]_{\text{sym}} \\ +\kappa(1-3\kappa')[2\mathbf{E}\mathbf{A}']_{\text{sym}} + (1-3\kappa)(1-3\kappa')I_{80}[\mathbf{M}\otimes\mathbf{M}']_{\text{sym}}\Big). \tag{58}$$

The quadruple contractions $4\mathbf{H}\bar{\otimes}\mathbf{H}' :: \mathbf{E}\otimes\mathbf{E}$ and $\mathbf{H}\bar{\otimes}\mathbf{H}' :: \mathbf{C}\otimes\mathbf{C}$ yield, respectively,

$$\begin{aligned}\hat{I}^{*}_{80} &= \kappa\kappa'(I_1^2 - 2I_2 - 2I_1 + 3) + \kappa'(1-3\kappa)(I_5 - 2I_4 + 1) \\ &\quad +\kappa(1-3\kappa')(I_7 - 2I_6 + 1) + (1-3\kappa)(1-3\kappa')\hat{I}_{80},\end{aligned} \tag{59}$$

$$\hat{I}^{*}_{8} = \kappa\kappa'(I_1^2 - 2I_2) + \kappa'(1-3\kappa)I_5 + \kappa(1-3\kappa')I_7 + (1-3\kappa)(1-3\kappa')\hat{I}_8, \tag{60}$$

where we used $2\mathbf{E} = \mathbf{C} - \mathbf{1}$, the definitions of invariants (1)–(4) and the identity $\mathbf{1} : \mathbf{C}^2 = I_1^2 - 2I_2$.

As expected, the strict alignment case $\hat{I}^{*}_{8} = \hat{I}_8$, $\hat{I}^{*}_{80} = \hat{I}_{80}$ is recovered for $\kappa = \kappa' = 0$. When one family is isotropic ($\kappa' = \frac{1}{3}$) invariants $\hat{I}^{\star}_{8}$ and $\hat{I}^{\star}_{80}$ capture the average values of invariants I_5 and $I_{50} = \mathbf{M}\otimes\mathbf{M} : (\mathbf{C}-\mathbf{1})^2$, $\hat{I}^{\star}_{8} = \frac{1}{3}I^{\star}_{5} = \frac{1}{3}\kappa(I_1^2 - 2I_2) + \frac{1}{3}(1-3\kappa)I_5$ and $\hat{I}^{\star}_{80} = \frac{1}{3}I^{\star}_{50} = \frac{1}{3}\left(\kappa\kappa'(I_1^2 - 2I_2 - 2I_1 + 3) + \kappa'(1-3\kappa)(I_5 - 2I_4 + 1)\right)$.

The elasticity tensor contributions can be computed by using (57) in (56).

3.3 Geometric interpretation of I_8 and related invariants

The I_8-like anisotropic invariants are defined as projections and can be expressed in terms of the cosines of angles between deformed structural directions. With $\cos\alpha_0 = \mathbf{M}\cdot\mathbf{M}'$ and $\cos\alpha = \mathbf{F}\mathbf{M}\cdot\mathbf{F}\mathbf{M}'$, we have

$$I_8 = \sqrt{I_4 I_6}\cos\alpha, \qquad I_{80} = \sqrt{I_4 I_6}\cos\alpha - \cos\alpha_0, \tag{61}$$

$$\tilde{I}_8 = \sqrt{I_4 I_6}\cos\alpha\cos\alpha_0, \qquad \tilde{I}_{80} = \left(\sqrt{I_4 I_6}\cos\alpha - \cos\alpha_0\right)\cos\alpha_0, \tag{62}$$

$$\hat{I}_8 = I_4 I_6\cos^2\alpha, \qquad \hat{I}_{80} = \left(\sqrt{I_4 I_6}\cos\alpha - \cos\alpha_0\right)^2. \tag{63}$$

These expressions allow us to interpret I_8-like invariants geometrically: they capture the angle between two structural directions along with their lengths, or the change thereof. One can consider a strain energy term that depends on the cosine of the angle alone (e.g., as in [26, 20]),

$$\psi(\mathring{I}_{80}), \qquad \mathring{I}_{80} = \frac{I_8}{\sqrt{I_4 I_6}} - I_9 = \cos\alpha - \cos\alpha_0. \tag{64}$$

This invariant, unlike the ones considered previously, cannot be factorised into structural and deformation parts, and cannot be expressed in terms of a structure tensor contracted with a deformation dependent part. This precludes the direct application of the GST approach. Also, there are no reasonable special cases that yield $\mathring{I}_{80} \equiv I_{80}$, because demanding $I_4(\mathbf{N})I_6(\mathbf{N}') = 1$ for a non-degenerate set of orientations leads to the trivial case of pure rotation, $\mathbf{F}^T\mathbf{F} = \mathbf{1}$.

Remark 4. The dispersed invariant $\hat{I}^{\star}_{80}$ incorporates fibre dispersion by averaging $\hat{I}_{80}$ with respect to orientation density functions of fibre families. Fibre dispersion can also be included into the

I_8-like term by defining $\hat{I}_{80}^{\circledast} = \left(\sqrt{I_4^\star I_6^\star}\cos\alpha - \cos\alpha_0\right)^2$. This invariant takes into account fibre splay only for computing mean square of stretch in fibre families, while the angles α and α_0 are calculated based on the mean fibre directions (in contrast to $\hat{I}_{80}^\star$, which considers angles between pairwise combinations of fibres from different families). Even though $\hat{I}_{80}^{\circledast}$ might seem a simpler alternative to $\hat{I}_{80}^\star$, we reject it for the following reasons. First, we do not see any particular justification for treating extensional and angular components differently for the purpose of averaging. Second, the notion of mean fibre direction is not applicable to a general ODF, in which case $\hat{I}_{80}^{\circledast}$ is not defined. Finally, a model based on $\hat{I}_{80}^{\circledast}$ displays a less complex behaviour. In Section 4.1 we show how fibre dispersion in invariant $\hat{I}_{80}^\star$ may reduce symmetry of a material with orthogonal mean fibre directions, as it indirectly involves anisotropic invariants I_5 and I_7. This is not the case for $\hat{I}_{80}^{\circledast}$, which depends on deformation only through I_1, I_4, I_6, and I_8.

4 Example. Application to a myocardium model

We illustrate the application of the GST approach to the I_8-term using the Holzapfel–Ogden model [5] for passive myocardium as an example. This model distinguishes three mutually orthogonal material directions in the reference configuration: the myofibre direction $\mathbf{f}_0$, the sheet direction $\mathbf{s}_0$, and the sheet-normal direction $\mathbf{n}_0$. The mechanical response of the tissue is defined by the strain-energy function

$$\Psi_{\mathrm{HO}} = \psi_{\mathrm{iso}}(I_1) + \psi_{\mathrm{f}}(I_{4\mathrm{f}}) + \psi_{\mathrm{s}}(I_{4\mathrm{s}}) + \psi_{\mathrm{fs}}(\hat{I}_{80\mathrm{fs}}), \tag{65}$$

where

$$\psi_{\mathrm{iso}}(I_1) = \frac{a}{2b}\left\{\exp[b(I_1 - 3)] - 1\right\}, \quad \psi_{\mathrm{fs}}(\hat{I}_{80\mathrm{fs}}) = \frac{a_{\mathrm{fs}}}{2b_{\mathrm{fs}}}\left\{\exp(b_{\mathrm{fs}}\hat{I}_{80\mathrm{fs}}) - 1\right\}, \tag{66}$$

$$\psi_i(I_{4i}) = \frac{a_i}{2b_i}\left\{\exp[b_i(I_{4i} - 1)^2] - 1\right\}, \; i = \mathrm{f}, \mathrm{s}, \tag{67}$$

and $I_{4\mathrm{f}} = \mathbf{f}_0 \cdot \mathbf{C}\mathbf{f}_0$, $I_{4\mathrm{s}} = \mathbf{s}_0 \cdot \mathbf{C}\mathbf{s}_0$, and $\hat{I}_{80\mathrm{fs}} \equiv \hat{I}_{8\mathrm{fs}} = (\mathbf{f}_0 \cdot \mathbf{C}\mathbf{s}_0)^2$, since $\mathbf{f}_0 \cdot \mathbf{s}_0 = 0$. A modification of this model, which was considered in [14, 15], is defined by

$$\Psi_{\mathrm{EPPH}} = \psi_{\mathrm{iso}}(I_1) + \psi_{\mathrm{f}}(I_{4\mathrm{f}}^\star) + \psi_{\mathrm{s}}(I_{4\mathrm{s}}^\star) + \psi_{\mathrm{fs}}(\hat{I}_{80\mathrm{fs}}), \tag{68}$$

where the dispersed invariants $I_{4i}^\star = \kappa_i I_1 + (1 - 3\kappa_i)I_4$, $i = \mathrm{f}, \mathrm{s}$ take into account axisymmetric distributions of two structural directions around their mean values, $\mathbf{f}_0$ and $\mathbf{s}_0$ (the notation Ψ_{EPPH} is due to first letters of the authors' names [14]). The extent of dispersion is controlled by parameters $0 \leq \kappa_{\mathrm{f}}, \kappa_{\mathrm{s}} \leq \frac{1}{3}$. The last term in the strain energy (68), which is responsible for fibre-sheet interaction, disregards fibre dispersion and is exactly the same, as in (65). We propose a model that accounts for fibre dispersion in *every* anisotropic term of the strain energy,

$$\Psi_{\mathrm{HO}}^\star = \psi_{\mathrm{iso}}(I_1) + \psi_{\mathrm{f}}(I_{4\mathrm{f}}^\star) + \psi_{\mathrm{s}}(I_{4\mathrm{s}}^\star) + \psi_{\mathrm{fs}}(\hat{I}_{80\mathrm{fs}}^\star), \tag{69}$$

where $\hat{I}_{80\mathrm{fs}}^\star$ is defined as in (60). Note that $\hat{I}_{80\mathrm{fs}}^\star \neq \hat{I}_{8\mathrm{fs}}^\star$, unless $\kappa_{\mathrm{f}} = \kappa_{\mathrm{s}} = 0$, and $\hat{I}_{80\mathrm{fs}}^\star$ is used here in view of the considerations in Remark 3. In order to observe the consequence of fibre dispersion in the mixed term alone, we also consider

$$\Psi_{\mathrm{HO8}}^\star = \psi_{\mathrm{iso}}(I_1) + \psi_{\mathrm{f}}(I_{4\mathrm{f}}) + \psi_{\mathrm{s}}(I_{4\mathrm{s}}) + \psi_{\mathrm{fs}}(\hat{I}_{80\mathrm{fs}}^\star). \tag{70}$$

The models are analysed and compared in simple shear and biaxial stretch, which approximate deformations in two common test protocols used for characterisation of the mechanical properties of soft tissues. For comparison we use a single parameter set [14], which is given in Table 1. All four models, HO, EPPH, HO8*, and HO*, are identical in the case of strict alignment of fibres ($\kappa_{\rm f} = \kappa_{\rm s} = 0$). The discrepancy between the models increases with the extent of dispersion, as demonstrated in what follows.

a	b	$a_{\rm f}$	$b_{\rm f}$	$a_{\rm s}$	$b_{\rm s}$	$a_{\rm fs}$	$b_{\rm fs}$	$\kappa_{\rm f}$	$\kappa_{\rm s}$
0.333	9.242	18.535	15.972	2.564	10.446	0.417	11.602	0.0886	0.0249

Table 1: Parameter values for Holzapfel–Ogden model for myocardium [5], which were provided in [14] to fit the shear experimental data from [6]. Parameters a, $a_{\rm f}$, $a_{\rm s}$, $a_{\rm fs}$ have dimensions of stress (kPa, hereinafter omitted), while parameters b, $b_{\rm f}$, $b_{\rm s}$, $b_{\rm fs}$ are dimensionless. The values for structural parameters $\kappa_{\rm f}$ and $\kappa_{\rm s}$ are estimated in [14]: $\kappa_{\rm f}$ corresponds to a diseased myocardium; sheet dispersion datum was not available for the diseased case, therefore the value of $\kappa_{\rm s}$ for the healthy case is used.

4.1 Simple shear

Six different deformations are defined by spatially uniform deformation gradients $\mathbf{F}_{\rm fs}$, $\mathbf{F}_{\rm fn}$, $\mathbf{F}_{\rm sf}$, $\mathbf{F}_{\rm sn}$, $\mathbf{F}_{\rm nf}$, $\mathbf{F}_{\rm ns}$, e.g., $\mathbf{F}_{\rm fs} = \mathbf{1} + \gamma \mathbf{s}_0 \otimes \mathbf{f}_0$, where γ is the amount of shear. For each deformation mode, consider a corresponding shear component of the Cauchy stress tensor, that is, for $\mathbf{F}_{\rm fs}$ consider $\sigma_{\rm fs} = \mathbf{f}_0 \cdot \boldsymbol{\sigma}(\mathbf{F}_{\rm fs}(\gamma))\mathbf{s}_0$ and so on. Detailed analytical expressions for the Cauchy stress in simple shear are derived in Appendix C. The resulting stress-strain curves, one for each deformation mode, are widely used to match forces and displacements measured in shear experiments (for instance, see [6, 5]), although it is commonly known that the uniform simple shear deformation cannot be maintained in principle in the standard experimental protocol, in which forces are applied to only two faces of a cuboidal sample.

The EPPH model (68) predicts values of $\sigma_{\rm fs}$ and $\sigma_{\rm sf}$ that are 22% and 43% higher than those predicted by the HO* model (69), Figure 2a. This indicates that accounting for fibre dispersion in the invariant $\hat{I}^\star_{80}$ can lead to significant changes in mechanical response. A comparison of the models (65)–(70) reveals that accounting for dispersion in anisotropic invariants leads to a softer material response, when the same set of material parameters is used. This "softening" effect of dispersion is greater in invariants $I^\star_{4\rm f}$ and $I^\star_{4\rm s}$ than in $\hat{I}^\star_{80\rm fs}$, Figure 2b. The stress curves with and without dispersion diverge due to the difference between the values of $\hat{I}^\star_{80\rm fs}$ and $\hat{I}_{80\rm fs}$ (Figure 4a) and the values of $\partial \hat{I}^\star_{80\rm fs}/\partial \mathbf{C}$ and $\partial \hat{I}^\star_{80\rm fs}/\partial \mathbf{C}$.

Incorporating fibre dispersion into the mixed term $\psi_{\rm fs}$ also reduces the symmetry of the material. The original HO model (65) and the EPPH model (68) predict identical shear response in nf and ns modes, whereas the HO* model (69) permits distinct behaviour. This can be explained by noting that $I^\star_{80}$ is no longer invariant under permutation f $\leftrightarrow$ s, if only the two associated distributions are not identical, see equation (59) and Figure 1. The identity (59) also shows that the strain energy (69) indirectly involves more anisotropic invariants, compared to strain energy (68). One can expect more anisotropy in a material characterised by a greater number of anisotropic invariants. The difference $|\sigma_{\rm nf} - \sigma_{\rm ns}|$ increases as a monotonic function of $|\kappa_{\rm f} - \kappa_{\rm s}|$, as illustrated in Figure 3. Some of the data reported in [6] shows clearly distinct behaviour of myocardium in nf and ns modes, but the values of the dispersion parameters presently used are too low to account for it within the HO* model (69).

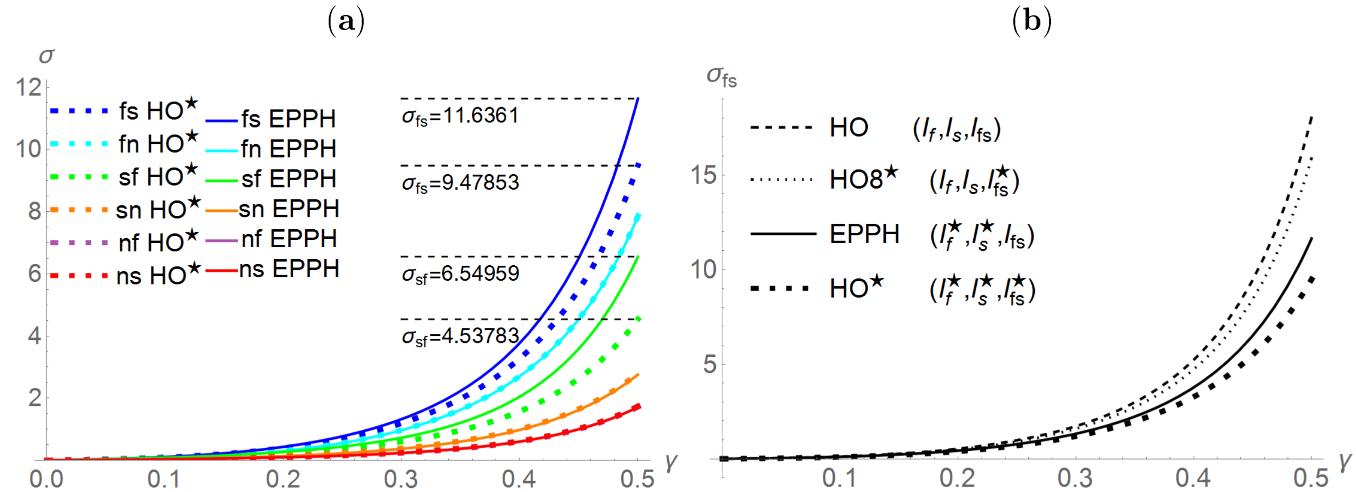

Figure 2: Softening effect of orientational dispersion. (a) Shear stress as a function of amount of shear in 6 shear modes as predicted by the EPPH model (68) [14] (solid) and the proposed model HO* (69) (dashed). (b) Shear stress σ_{fs} in the corresponding shear mode, as predicted by the original HO model (65), EPPH model (68), the proposed HO* model (69), which takes into account dispersion in all terms, and the model HO8* (70), which considers dispersion only in the invariant $\hat{I}^\star_{80}$.

4.2 Biaxial stretch

The effect of dispersion in $\hat{I}^\star_{80}$ is small in biaxial stretch deformations, which are defined as $\mathbf{F}_{\mathrm{biax}} = \lambda_1 \mathbf{f}_0 \otimes \mathbf{f}_0 + \lambda_2 \mathbf{s}_0 \otimes \mathbf{s}_0 + \lambda_1^{-1}\lambda_2^{-1} \mathbf{n}_0 \otimes \mathbf{n}_0$, where the principal stretches are related by the ratio $r = (\lambda_1 - 1)\,/\,(\lambda_2 - 1)$, and the boundary condition $\boldsymbol{\sigma} \cdot \mathbf{n}_0 = \mathbf{0}$ is implied. Detailed analytical expressions for the Cauchy stress are derived in Appendix C. In the strict alignment case, we have $\hat{I}^\star_{80} \equiv \hat{I}_{80} = 0$, as the deformation is coaxial with the structural directions $\mathbf{f}_0$, $\mathbf{s}_0$, and $\mathbf{n}_0$, which remain orthogonal in the deformed state. In the presence of orientational dispersion, the integrated fibre directions $\mathbf{N}$ and $\mathbf{N}'$ are almost always (in the probability-theoretical sense) non-orthogonal in both the reference and current configurations, as shown in Figure 1b. This leads to a non-zero value of $\hat{I}^\star_{80}$ and engages the mixed term ψ_{fs} into the stress response under biaxial stretching. Notwithstanding, the value of $\hat{I}^\star_{80}$ remains very small (Figure 4b), and the effect on the stress curves is negligible for the parameter values given in Table 1. Note that the considered ranges of shear and biaxial deformations are consistent in the sense that stress values of the same order are recorded for them in experiments [7].

One can also consider a biaxial deformation that is not coaxial with the structural directions $\mathbf{f}_0$, $\mathbf{s}_0$, i.e. rotated around $\mathbf{n}_0$. In this case, both $\hat{I}_{80}$ and $\hat{I}^\star_{80}$ are non-zero under a non-equibiaxial stretch. Nevertheless, their values remain small and the effect of dispersion in $\hat{I}^\star_{80}$ is negligible under the biaxial stretching. This can be seen by computing the maximum value of I_{80} with respect to the rotating orthogonal axes $\{\mathbf{f}_0, \mathbf{s}_0\}$ or the maximum shear component of $2\mathbf{E}_{\mathrm{biax}} = (\lambda_1^2 - 1)\mathbf{E}_1 \otimes \mathbf{E}_1 + (\lambda_2^2 - 1)\mathbf{E}_2 \otimes \mathbf{E}_2 + (\lambda_1^{-2}\lambda_2^{-2} - 1)\mathbf{n}_0 \otimes \mathbf{n}_0$, which is the same and is given by $I_{80\max} = \frac{1}{2}\,(\lambda_1^2 - \lambda_2^2)$. For the protocols used in [7], $I_{80\max} = 0.05375$ is attained at $\lambda = 1.1$, $r = 2$ and is one order of magnitude smaller than the value in the fs-shear deformation mode, $I_{80\max} = \gamma_{\max} = 0.5$. Therefore, the contribution of $\psi_{\mathrm{fs}}(\hat{I}^\star_{80})$ itself is not significant in biaxial stretch, not to mention the effect of dispersion in this mixed term.

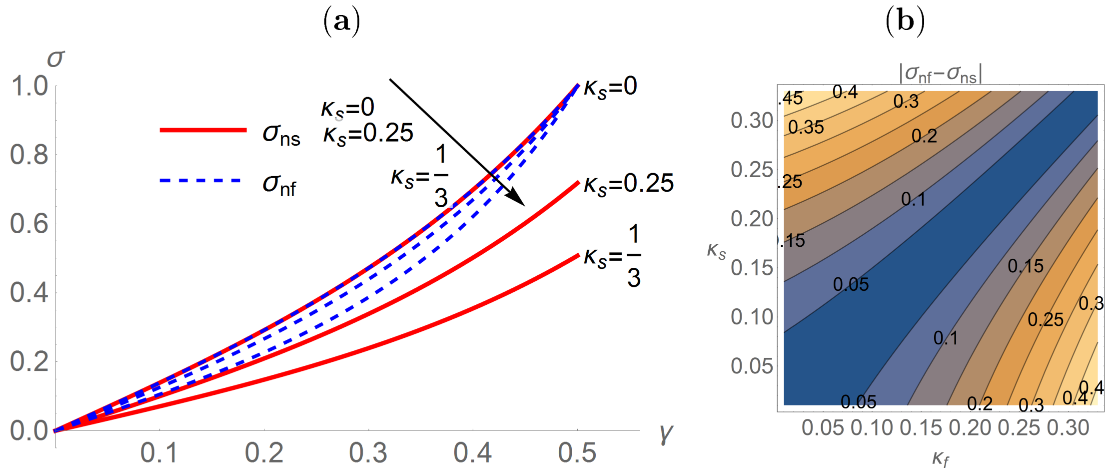

Figure 3: The HO* model (69) allows distinct response in the nf and ns shear deformation modes. (a) Shear stresses $\sigma_{\rm nf}$ and $\sigma_{\rm ns}$ in the respective modes plotted for selected values of $\kappa_{\rm s}$ (the arrow shows the order of $\sigma_{\rm nf}$ curves as $\kappa_{\rm s}$ increases). The value of a is chosen to satisfy $\sigma_{\rm nf}|_{\gamma=0.5}=1$, while other parameters are fixed, $\kappa_{\rm f}=a_{\rm f}=a_{\rm s}=0$, $b=1.5$, $a_{\rm fs}=1$, $b_{\rm fs}=13$. (b) The value of $|\sigma_{\rm nf}-\sigma_{\rm ns}|$ at $\gamma=0.5$ in respective deformation modes as a function of $\kappa_{\rm f}$ and κ_s; other parameters are as in (a). Both plots demonstrate that the difference $|\sigma_{\rm nf}-\sigma_{\rm ns}|$ increases together with $|\kappa_{\rm f}-\kappa_s|$.

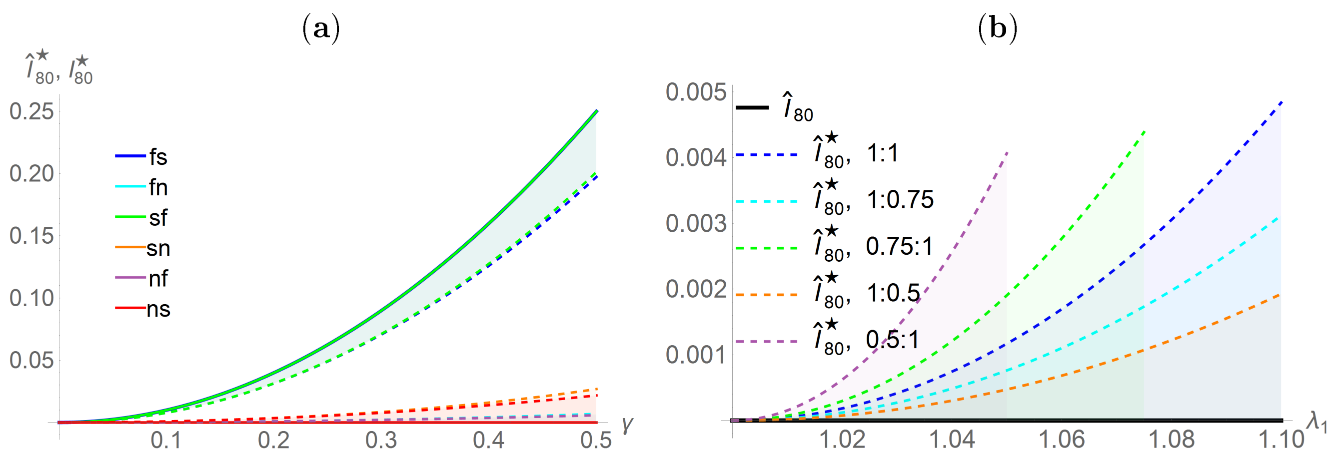

Figure 4: Invariants $\hat{I}^\star_{80}$ (dashed) and $\hat{I}_{80}$ (solid) in simple shear (a) and biaxial stretch (b). Shaded area depicts the difference $\hat{I}^\star_{80}-\hat{I}_{80}$ in respective deformation modes. The effect of dispersion for dispersion values $\kappa_{\rm f}=0.086$, $\kappa_{\rm s}=0.0249$ is substantial in simple shear, but insignificant in biaxial stretch.

5 Discussion

We have applied the GST approach for materials with orientationally distributed fibres to strain-energy functions that depend on the coupling invariant I_8, which represent pairwise interaction between fibre families. By analogy with the original GST model for I_4 and its extension for I_5 [4, 11], we have considered the weighted averages of invariants $\tilde{I}_8=I_8I_9$ and $\hat{I}_8=I_8^2$ and derived two corresponding GST formulations. With our contribution, one can properly incorporate fibre dispersion data into material models that include invariant I_8 and, in principle, into any hyperelastic constitutive model, since GST-based expressions are now available for every anisotropic invariant in the set $I_1, \ldots, I_9$, which forms a functional basis for an arbitrary strain-energy function [21, 22].

Using the Holzapfel–Ogden model for passive myocardium [5] as an example, we have demonstrated that accounting for fibre dispersion in the coupled term can have a significant quantitative effect in shearing deformations (Figure 2). This indicates that the models that ignore fibre dispersion in this term [14] may predict behaviour inconsistent with their basic assumptions and need to be reassessed or modified in the fashion we propose. The proposed HO* model and the models that ignore fibre dispersion in some or all terms fit shear test data [6] equally well for a range of structural parameters, when the tissue is idealised as a homogeneously deformed uniform body (not shown). However, depending on the values of fibre and sheet dispersion parameters, the proposed model is capable of more complex anisotropic response, which we discuss next. It must be noted that inhomogeneous deformations and variability of tissue structure across a test specimen, as well as proper boundary conditions, should be taken into account when fitting a model to experimental data. In general, this can only be done by solving the corresponding boundary value problem numerically, e.g., using finite element methods.

The incorporation of fibre dispersion in the coupling invariant, unlike that in other anisotropic invariants, has a potential to reduce material symmetry, when the extent of dispersion varies between the fibre families (Figure 3). This effect is minor for the parameter values used here (Table 1, [14]): the phenomenological constitutive parameters were fitted to simple shear behaviour of porcine myocardium (with no record of abnormality) [6], while the dispersion parameters correspond to hypertrophic fibre and normal laminar murine myocardial structures [27, 28, 14]. New data and further studies are required to estimate the relevance of this reduced material symmetry in diseased myocardium and other tissues, where the effect of fibre dispersion in the coupling invariant can potentially be significant and sufficient to explain increased mechanical anisotropy without need for extra terms of the strain-energy function or explicit dependence on additional anisotropic invariants.

It has been brought to our attention that the six shear modes of the HO* model (69) are not only distinct, but also do not satisfy the relation

$$\sigma_{\mathrm{fs}}(\gamma) + \sigma_{\mathrm{sn}}(\gamma) + \sigma_{\mathrm{nf}}(\gamma) = \sigma_{\mathrm{sf}}(\gamma) + \sigma_{\mathrm{ns}}(\gamma) + \sigma_{\mathrm{fn}}(\gamma), \tag{71}$$

which holds for the HO model (65) and the EPPH model (68). The relation (71) was noted by Latorre and Montans [29] for materials with the strain energy $\Psi_{\mathrm{LM}} = \sum_{i,j} \omega_{ij}(\mathcal{E}_{ij})$, where $\mathcal{E}_{ij}$ are the components of the logarithmic Lagrangian strain tensor $\boldsymbol{\mathcal{E}} = \ln \mathbf{E}$ and ω_{ij} are suitable (but otherwise arbitrary) spline functions. We note that condition (71) is ensured (for some materials) by the additive split $\Psi = \sum_i \psi_i(I_i)$, where each $\psi_i(I_i)$ is invariant with respect to at least one odd permutation of subscripts $(\mathrm{f}, \mathrm{s}, \mathrm{n})$. For example, in the case of axisymmetric fibre dispersion, the term $\psi_{\mathrm{f}}(I^\star_{4\mathrm{f}})$ is invariant with respect to permutation $(\mathrm{f}, \mathrm{s}, \mathrm{n}) \mapsto (\mathrm{f}, \mathrm{n}, \mathrm{s})$. It follows and can be rigourously demonstrated that a bijection is established between the contributions of ψ_{f} to the Cauchy stresses on the opposite sides of condition (71). Therefore, for a material model to satisfy condition (71), it is sufficient that each additive term of its strain energy function respects some odd permutation of subscripts $(\mathrm{f}, \mathrm{s}, \mathrm{n})$. The condition (71) does not hold for the HO* model (69), because the mixed term $\psi_{\mathrm{fs}}(\hat{I}^\star_{8 0\mathrm{fs}})$ is affected by every odd permutation, with the only exception being $\kappa_{\mathrm{f}} = \kappa_{\mathrm{s}}$, as can be seen from equation (59), which should be changed beforehand to adopt notation used for myocardium.

It is often assumed that fibres buckle under compression and only contribute to material response when stretched. Constitutive models address this assumption by excluding compressed fibres by means of switch conditions [4, 30], deformation-dependent [31] or pre-integrated GSTs [12, 32]. These studies consider exclusion of compressed fibres in the context of decoupled fibre families, whose elastic potentials are functions of I_4. Avazmohammadi et al. [33] considered a fibre interaction term, which vanishes as soon as one fibre family is slack. Their model captures the coupling between fibre families using a linear combination of I_4-like invariants. Even though the relevance of fibre exclusion to invariant I_8 remains to be examined from the physical standpoint and also considering material stability [24], all existing methods for fibre exclusion can be straightforwardly applied to the proposed formulations, since the fourth-order GST $\hat{\mathbb{H}}$ and the structure-like tensor $\tilde{\mathbf{H}}$ are defined in terms of the second-order GSTs.

6 Conclusion

We have derived two GST formulations for invariants $\hat{I}_8$ and $\tilde{I}_8$, which capture the pair-wise coupling of fibre families in a fibre-reinforced material. With this method, orientational distribution of fibres can be incorporated into the coupling part of a hyperelastic constitutive model. Although we have used a model for myocardium as an example, the method is general and can be applied to any soft tissue. The following theoretical observations have been made in the course of derivation. We have noted that I_8 cannot be used as a basis of a GST model, since it is an odd function of structural directions. We have also noted that in order to formulate a universal constitutive law applicable to various material structures, the averaging must be applied not to $\hat{I}_8$ or $\tilde{I}_8$ directly, but to their strain-based counterparts, $\hat{I}_{80}$ and $\tilde{I}_{80}$. The resulting models can be expressed in terms of a fourth-order structure and second-order structure-like tensors, respectively, which in turn are given by a tensor and dot products of the well-known GSTs. Simpler expressions are available for the case of axisymmetric fibre distributions.

We have applied our formulation to the Holzapfel–Ogden model for myocardium [5] and obtained a model, which takes into account fibre dispersion in every term of the strain-energy function. We have shown that including fibre dispersion in the coupling term significantly decreases the stress in simple shear deformations and also causes minor changes in biaxial stretching. In addition, the proposed model can produce six distinct response curves, which correspond to six simple shear modes, whereas in models without dispersion in the coupling term [5, 14] two curves coincide exactly. This loss of symmetry is negligible for the parameter set that we used for myocardium, but just like the effect on biaxial response, it can be significant for other parameter values or in other tissues. We conclude that the proposed model should be used instead of the models we compared it to [5, 14], because it consistently incorporates fibre dispersion in every term of the strain-energy function and can predict quantitatively and qualitatively different behaviour.

Acknowledgements

This study was supported by Engineering and Physical Sciences Research Council (EPSRC) of the UK (grant reference number EP/N014642/1) and was conducted at SofTMech, the EPSRC Centre for Multiscale Soft Tissue Mechanics. We would like to thank reviewers, whose remarks helped to improve the presentation of this work and led to discussion included in Remark 4 and parts of Sections 4.2 and 5.

References

[1] M. J. Unterberger, K. M. Schmoller, C. Wurm, A. R. Bausch, G. A. Holzapfel, Viscoelasticity of cross-linked actin networks: Experimental tests, mechanical modeling and finite-element analysis, Acta Biomaterialia 9 (7) (2013) 7343–7353. doi:10.1016/j.actbio.2013.03.008.

[2] A. Grytsan, P. N. Watton, G. A. Holzapfel, A thick-walled fluid–solid-growth model of abdominal aortic aneurysm evolution: Application to a patient-specific geometry, Journal of biomechanical engineering 137 (3) (2015) 031008.

[3] T. Shearer, A new strain energy function for the hyperelastic modelling of ligaments and tendons based on fascicle microstructure, Journal of Biomechanics 48 (2) (2015) 290–297. doi:10.1016/j.jbiomech.2014.11.031.

[4] T. C. Gasser, R. W. Ogden, G. A. Holzapfel, Hyperelastic modelling of arterial layers with distributed collagen fibre orientations., Journal of the Royal Society, Interface / the Royal Society 3 (6) (2006) 15–35. doi:10.1098/rsif.2005.0073.

[5] G. A. Holzapfel, R. W. Ogden, Constitutive modelling of passive myocardium: a structurally based framework for material characterization., Philosophical transactions. Series A, Mathematical, physical, and engineering sciences 367 (1902) (2009) 3445–75. doi:10.1098/rsta.2009.0091.

[6] S. Dokos, B. H. Smaill, A. A. Young, I. J. LeGrice, Shear properties of passive ventricular myocardium., American journal of physiology. Heart and circulatory physiology 283 (6) (2002) H2650–H2659. doi:10.1152/ajpheart.00111.2002.

[7] G. Sommer, A. J. Schriefl, M. Andrä, M. Sacherer, C. Viertler, H. Wolinski, G. A. Holzapfel, Biomechanical properties and microstructure of human ventricular myocardium, Acta Biomaterialia 24 (2015) 172–192. doi:10.1016/j.actbio.2015.06.031.

[8] A. J. Schriefl, H. Wolinski, P. Regitnig, S. D. Kohlwein, G. A. Holzapfel, An automated approach for three-dimensional quantification of fibrillar structures in optically cleared soft biological tissues., Journal of the Royal Society, Interface / the Royal Society 10 (80) (2013) 20120760. doi:10.1098/rsif.2012.0760.

[9] Y. Lanir, Constitutive equations for fibrous connective tissues, Journal of Biomechanics 16 (1) (1983) 1–12. doi:10.1016/0021-9290(83)90041-6.

[10] A. D. Freed, D. R. Einstein, I. Vesely, Invariant formulation for dispersed transverse isotropy in aortic heart valves, Biomechanics and modeling in mechanobiology 4 (2-3) (2005) 100–117.

[11] G. A. Holzapfel, R. W. Ogden, Comparison of two model frameworks for fiber dispersion in the elasticity of soft biological tissues, European Journal of Mechanics-A/Solids 66 (2017) 193–200.

[12] G. A. Holzapfel, R. W. Ogden, On fiber dispersion models: Exclusion of compressed fibers and spurious model comparisons, Journal of Elasticity (2016) 1–20.

[13] G. A. Holzapfel, R. W. Ogden, Constitutive modelling of arteries, Proceedings of the Royal Society A: Mathematical, Physical and Engineering Sciences 466 (2118) (2010) 1551–1597. doi:10.1098/rspa.2010.0058.

[14] T. S. Eriksson, A. J. Prassl, G. Plank, G. A. Holzapfel, Modeling the dispersion in electromechanically coupled myocardium, International journal for numerical methods in biomedical engineering 29 (11) (2013) 1267–1284.

[15] O. Gültekin, G. Sommer, G. A. Holzapfel, An orthotropic viscoelastic model for the passive myocardium: continuum basis and numerical treatment, Computer Methods in Biomechanics and Biomedical Engineering (2016) 1–18doi:10.1080/10255842.2016.1176155.

[16] S. Federico, T. C. Gasser, Nonlinear elasticity of biological tissues with statistical fibre orientation, Journal of the Royal Society Interface 7 (47) (2010) 955–966.

[17] D. M. Pierce, W. Trobin, J. G. Raya, S. Trattnig, H. Bischof, C. Glaser, G. A. Holzapfel, DT-MRI based computation of collagen fiber deformation in human articular cartilage: A feasibility study, Annals of Biomedical Engineering 38 (7) (2010) 2447–2463. doi:10.1007/s10439-010-9990-9.

[18] Z. Guo, X. Shi, X. Peng, F. Caner, Fibre–matrix interaction in the human annulus fibrosus, Journal of the mechanical behavior of biomedical materials 5 (1) (2012) 193–205.

[19] A. Pandolfi, G. A. Holzapfel, Three-dimensional modeling and computational analysis of the human cornea considering distributed collagen fibril orientations., Journal of biomechanical engineering 130 (6) (2008) 061006. doi:10.1115/1.2982251.

[20] N. L. Nerurkar, R. L. Mauck, D. M. Elliott, Modeling interlamellar interactions in angle-ply biologic laminates for annulus fibrosus tissue engineering, Biomechanics and modeling in mechanobiology 10 (6) (2011) 973–984.

[21] A. S. Wineman, A. Pipkin, Material symmetry restrictions on constitutive equations, Archive for Rational Mechanics and Analysis 17 (3) (1964) 184–214.

[22] A. Spencer, Theory of invariants, Continuum Phys. 1 (1971) 239–353.

[23] A. J. M. Spencer, Constitutive theory for strongly anisotropic solids, in: Continuum theory of the mechanics of fibre-reinforced composites, Springer, 1984, pp. 1–32.

[24] J. Merodio, R. W. Ogden, The influence of the invariant I8 on the stress-deformation and ellipticity characteristics of doubly fiber-reinforced non-linearly elastic solids, International Journal of Non-Linear Mechanics 41 (4) (2006) 556–563. doi:10.1016/j.ijnonlinmec.2006.02.001.

[25] G. Chagnon, M. Rebouah, D. Favier, Hyperelastic energy densities for soft biological tissues: a review, Journal of Elasticity 120 (2) (2015) 129–160.

[26] X. Peng, Z. Guo, T. Du, W.-R. Yu, A simple anisotropic hyperelastic constitutive model for textile fabrics with application to forming simulation, Composites Part B: Engineering 52 (2013) 275–281.

[27] W. J. Karlon, J. W. Covell, A. D. Mcculloch, J. J. Hunter, J. H. Omens, Automated measurement of myofiber disarray in transgenic mice with ventricular expression of ras, The Anatomical Record 252 (4) (1998) 612–625.

[28] G. B. Sands, B. H. Smaill, I. J. LeGrice, Virtual sectioning of cardiac tissue relative to fiber orientation, in: Engineering in Medicine and Biology Society, 2008. EMBS 2008. 30th Annual International Conference of the IEEE, IEEE, 2008, pp. 226–229.

[29] M. Latorre, F. J. Montáns, Wypiwyg hyperelasticity without inversion formula: Application to passive ventricular myocardium, Computers & Structures 185 (2017) 47–58.

[30] G. A. Holzapfel, R. W. Ogden, On the tension-compression switch in soft fibrous solids, European Journal of Mechanics, A/Solids 49 (2015) 561–569. doi:10.1016/j.euromechsol.2014.09.005.

[31] A. V. Melnik, H. Borja Da Rocha, A. Goriely, On the modeling of fiber dispersion in fiber-reinforced elastic materials, International Journal of Non-Linear Mechanics 75 (2015) 92–106. doi:10.1016/j.ijnonlinmec.2014.10.006.

[32] M. Latorre, F. J. Montáns, On the tension-compression switch of the Gasser-Ogden-Holzapfel model: Analysis and a new pre-integrated proposal, Journal of the Mechanical Behavior of Biomedical Materials 57 (2016) 175–189. doi:10.1016/j.jmbbm.2015.11.018.

[33] R. Avazmohammadi, M. R. Hill, M. A. Simon, W. Zhang, M. S. Sacks, A novel constitutive model for passive right ventricular myocardium: evidence for myofiber–collagen fiber mechanical coupling, Biomechanics and modeling in mechanobiology 16 (2) (2017) 561–581.

A Appendix A. An expression for I_8^2 in an orthotropic material

Lemma 1. *We demonstrate that*

$$0 = I_2 + I_5 + I_7 + I_4 I_6 - I_1 (I_4 + I_6) - I_8^2, \tag{72}$$

if only unit vectors $\mathbf{M}$ *and* $\mathbf{M}'$ *in (1)–(5) are orthogonal, i.e.* $\mathbf{M} \cdot \mathbf{M}' = 0$.

Proof. We introduce notation $\mathbf{A} = \mathbf{M} \otimes \mathbf{M}$, $\mathbf{A}' = \mathbf{M}' \otimes \mathbf{M}'$, $\mathbf{A}'' = \mathbf{M}'' \otimes \mathbf{M}''$, where $\mathbf{M}''$ is a unit vector, orthogonal to both $\mathbf{M}$ and $\mathbf{M}'$. From these definitions if follows that

$$\mathbf{A} \otimes \mathbf{A} = \mathbf{A} \bar{\otimes} \mathbf{A}, \quad \mathbf{A}' \otimes \mathbf{A}' = \mathbf{A}' \bar{\otimes} \mathbf{A}', \quad \mathbf{A}'' \otimes \mathbf{A}'' = \mathbf{A}'' \bar{\otimes} \mathbf{A}''. \tag{73}$$

Orthonormality of $\mathbf{M}$ and $\mathbf{M}'$ implies that $\{\mathbf{M}, \mathbf{M}', \mathbf{M}''\}$ is an orthonormal basis, therefore,

$$\mathbf{1} = \mathbf{A} + \mathbf{A}' + \mathbf{A}''. \tag{74}$$

For the terms involved in (72) we have the following,

$$I_2 = \frac{1}{2} (\mathbf{1} \otimes \mathbf{1} - \mathbf{1} \bar{\otimes} \mathbf{1}) :: \mathbf{C} \otimes \mathbf{C} \tag{75}$$

$$I_5 = \mathbf{A} \bar{\otimes} \mathbf{1} :: \mathbf{C} \otimes \mathbf{C}, \qquad I_7 = \mathbf{A}' \bar{\otimes} \mathbf{1} :: \mathbf{C} \otimes \mathbf{C}, \tag{76}$$

$$I_4 I_6 = (\mathbf{A} : \mathbf{C})(\mathbf{A}' : \mathbf{C}) = \mathbf{A} \otimes \mathbf{A}' :: \mathbf{C} \otimes \mathbf{C}, \tag{77}$$

$$I_1 I_4 = \mathbf{1} \otimes \mathbf{A} :: \mathbf{C} \otimes \mathbf{C}, \qquad I_1 I_6 = \mathbf{1} \otimes \mathbf{A}' :: \mathbf{C} \otimes \mathbf{C}, \tag{78}$$

$$I_8^2 = \mathbf{A} \bar{\otimes} \mathbf{A}' :: \mathbf{C} \otimes \mathbf{C}. \tag{79}$$

Now we need to demonstrate that

$$\left(\frac{1}{2} (\mathbf{1} \otimes \mathbf{1} - \mathbf{1} \bar{\otimes} \mathbf{1}) + \mathbf{A} \bar{\otimes} \mathbf{1} + \mathbf{A}' \bar{\otimes} \mathbf{1} + \mathbf{A} \otimes \mathbf{A}' - \mathbf{1} \otimes \mathbf{A} - \mathbf{1} \otimes \mathbf{A}' - \mathbf{A} \bar{\otimes} \mathbf{A}' \right) :: \mathbf{C} \otimes \mathbf{C} = 0.$$

It is sufficient to show that

$$\frac{1}{2} (\mathbf{1} \otimes \mathbf{1} - \mathbf{1} \bar{\otimes} \mathbf{1}) + \mathbf{A} \bar{\otimes} \mathbf{1} + \mathbf{A}' \bar{\otimes} \mathbf{1} + \mathbf{A} \otimes \mathbf{A}' - \mathbf{1} \otimes \mathbf{A} - \mathbf{1} \otimes \mathbf{A}' - \mathbf{A} \bar{\otimes} \mathbf{A}' = \mathbf{0} \otimes \mathbf{0}, \tag{80}$$

up to the major symmetry, in the sense that respects identification $\mathbf{A} \otimes \mathbf{A}' \equiv \mathbf{A}' \otimes \mathbf{A}$, $\mathbf{A} \bar{\otimes} \mathbf{A}' \equiv \mathbf{A}' \bar{\otimes} \mathbf{A}$, etc. To proceed, we replace $\mathbf{1}$ via (74). The first term, up to the major symmetry, becomes

$$\begin{aligned} \frac{1}{2} (\mathbf{1} \otimes \mathbf{1} - \mathbf{1} \bar{\otimes} \mathbf{1}) &= \frac{1}{2} \left((\mathbf{A} + \mathbf{A}' + \mathbf{A}'') \otimes (\mathbf{A} + \mathbf{A}' + \mathbf{A}'') - (\mathbf{A} + \mathbf{A}' + \mathbf{A}'') \bar{\otimes} (\mathbf{A} + \mathbf{A}' + \mathbf{A}'') \right) \\ &= \mathbf{A} \otimes \mathbf{A}' + \mathbf{A} \otimes \mathbf{A}'' + \mathbf{A}' \otimes \mathbf{A}'' - \mathbf{A} \bar{\otimes} \mathbf{A}' - \mathbf{A} \bar{\otimes} \mathbf{A}'' - \mathbf{A}' \bar{\otimes} \mathbf{A}'', \end{aligned} \tag{81}$$

where identities (73) were employed. Next,

$$\begin{aligned} \mathbf{A} \bar{\otimes} \mathbf{1} + \mathbf{A}' \bar{\otimes} \mathbf{1} - \mathbf{A} \bar{\otimes} \mathbf{A}' &= (\mathbf{A} \bar{\otimes} \mathbf{A} + \mathbf{A} \bar{\otimes} \mathbf{A}' + \mathbf{A}' \bar{\otimes} \mathbf{A}'') + (\mathbf{A}' \bar{\otimes} \mathbf{A} + \mathbf{A}' \bar{\otimes} \mathbf{A}' + \mathbf{A}' \bar{\otimes} \mathbf{A}'') - \mathbf{A} \bar{\otimes} \mathbf{A}' \\ &= \mathbf{A} \otimes \mathbf{A} + \mathbf{A}' \otimes \mathbf{A}' + \mathbf{A} \bar{\otimes} \mathbf{A}' + \mathbf{A} \bar{\otimes} \mathbf{A}'' + \mathbf{A}' \bar{\otimes} \mathbf{A}'', \end{aligned} \tag{82}$$

and similarly,

$$\begin{aligned} \mathbf{A} \otimes \mathbf{1} + \mathbf{A}' \otimes \mathbf{1} - \mathbf{A} \otimes \mathbf{A}' &= \mathbf{A} \otimes \mathbf{A} + \mathbf{A} \otimes \mathbf{A}' + \mathbf{A} \otimes \mathbf{A}'' + \mathbf{A}' \otimes \mathbf{A} + \mathbf{A}' \otimes \mathbf{A}' + \mathbf{A}' \otimes \mathbf{A}'' - \mathbf{A} \otimes \mathbf{A}'' \\ &= \mathbf{A} \otimes \mathbf{A} + \mathbf{A}' \otimes \mathbf{A}' + \mathbf{A} \otimes \mathbf{A}' + \mathbf{A} \otimes \mathbf{A}'' + \mathbf{A}' \otimes \mathbf{A}''. \end{aligned} \tag{83}$$

After taking the sum of equations (81)–(83), one can clearly see that (80) holds. □

B Appendix B. Expressions for the case of coaxially aligned non-symmetrically dispersed families of fibres

Consider two coaxial GSTs, which are given by $\mathbf{H} = \mathrm{diag}(\mathrm{H}_{11}, \mathrm{H}_{22}, \mathrm{H}_{33})$, $\mathbf{H}' = \mathrm{diag}(\mathrm{H}'_{11}, \mathrm{H}'_{22}, \mathrm{H}'_{33})$ in an orthonormal basis $\{\mathbf{M}, \mathbf{M}', \mathbf{M}''\}$, that is,

$$\mathbf{H} = \mathrm{H}_{11}\mathbf{A} + \mathrm{H}_{22}\mathbf{A}' + \mathrm{H}_{33}(\mathbf{1} - \mathbf{A} - \mathbf{A}'), \quad \mathbf{H}' = \mathrm{H}'_{11}\mathbf{A} + \mathrm{H}'_{22}\mathbf{A}' + \mathrm{H}'_{33}(\mathbf{1} - \mathbf{A} - \mathbf{A}'), \tag{84}$$

with $\mathbf{A} = \mathbf{M}\otimes\mathbf{M}$, $\mathbf{A}' = \mathbf{M}'\otimes\mathbf{M}'$, $\mathbf{A}'' = \mathbf{M}''\otimes\mathbf{M}''$. A specialisation of equation (49) for this case reads

$$\hat{\mathbb{H}} = \mathrm{H}_{33}\mathrm{H}'_{33}\mathbf{1}\bar{\otimes}\mathbf{1} + (\mathrm{H}_{11} - \mathrm{H}_{33})(\mathrm{H}'_{11} - \mathrm{H}'_{33})\,\mathbf{A}\otimes\mathbf{A} + (\mathrm{H}_{22} - \mathrm{H}_{33})(\mathrm{H}'_{22} - \mathrm{H}'_{33})\,\mathbf{A}'\otimes\mathbf{A}' \tag{85}$$
$$+ (\mathrm{H}'_{33}(\mathrm{H}_{11} - \mathrm{H}_{33}) + \mathrm{H}_{33}(\mathrm{H}'_{11} - \mathrm{H}'_{33}))\,[\mathbf{A}\bar{\otimes}\mathbf{1}]_{\mathrm{sym}} + (\mathrm{H}'_{33}(\mathrm{H}_{22} - \mathrm{H}_{33}) + \mathrm{H}_{33}(\mathrm{H}'_{22} - \mathrm{H}'_{33}))\,[\mathbf{A}'\bar{\otimes}\mathbf{1}]_{\mathrm{sym}} \tag{86}$$
$$+ ((\mathrm{H}_{11} - \mathrm{H}_{33})(\mathrm{H}'_{22} - \mathrm{H}'_{33}) + (\mathrm{H}_{22} - \mathrm{H}_{33})(\mathrm{H}'_{11} - \mathrm{H}'_{33}))\,[\mathbf{A}\bar{\otimes}\mathbf{A}']_{\mathrm{sym}}\,. \tag{87}$$

Double contraction with $2\mathbf{E}$ yields

$$2\hat{\mathbb{H}} : \mathbf{E} = \mathrm{H}_{33}\mathrm{H}'_{33}\,(2\mathbf{E}) + (\mathrm{H}_{11} - \mathrm{H}_{33})(\mathrm{H}'_{11} - \mathrm{H}'_{33})\,(I_4 - 1)\,\mathbf{A} + (\mathrm{H}_{22} - \mathrm{H}_{33})(\mathrm{H}'_{22} - \mathrm{H}'_{33})\,(I_6 - 1)\,\mathbf{A}' \tag{88}$$
$$+ (\mathrm{H}'_{33}(\mathrm{H}_{11} - \mathrm{H}_{33}) + \mathrm{H}_{33}(\mathrm{H}'_{11} - \mathrm{H}'_{33}))\,[2\mathbf{E}\mathbf{A}]_{\mathrm{sym}} + (\mathrm{H}'_{33}(\mathrm{H}_{22} - \mathrm{H}_{33}) + \mathrm{H}_{33}(\mathrm{H}'_{22} - \mathrm{H}'_{33}))\,[2\mathbf{E}\mathbf{A}']_{\mathrm{sym}} \tag{89}$$
$$+ ((\mathrm{H}_{11} - \mathrm{H}_{33})(\mathrm{H}'_{22} - \mathrm{H}'_{33}) + (\mathrm{H}_{22} - \mathrm{H}_{33})(\mathrm{H}'_{11} - \mathrm{H}'_{33}))\,I_{80}\,[\mathbf{M}\otimes\mathbf{M}']_{\mathrm{sym}}\,. \tag{90}$$

Quadruple contraction with $4\mathbf{E}\otimes\mathbf{E}$ results in

$$\hat{I}^{\star}_{80} = \mathrm{H}_{33}\mathrm{H}'_{33}\,(I_1 - 2I_2 - 2I_2 + 3)^2 + (\mathrm{H}_{11} - \mathrm{H}_{33})(\mathrm{H}'_{11} - \mathrm{H}'_{33})\,(I_4 - 1)^2 + (\mathrm{H}_{22} - \mathrm{H}_{33})(\mathrm{H}'_{22} - \mathrm{H}'_{33})\,(I_6 - 1)^2 \tag{91}$$
$$+ (\mathrm{H}'_{33}(\mathrm{H}_{11} - \mathrm{H}_{33}) + \mathrm{H}_{33}(\mathrm{H}'_{11} - \mathrm{H}'_{33}))\,(I_5 - 2I_4 + 1) + (\mathrm{H}'_{33}(\mathrm{H}_{22} - \mathrm{H}_{33}) + \mathrm{H}_{33}(\mathrm{H}'_{22} - \mathrm{H}'_{33}))\,(I_7 - 2I_6 + 1) \tag{92}$$
$$+ ((\mathrm{H}_{11} - \mathrm{H}_{33})(\mathrm{H}'_{22} - \mathrm{H}'_{33}) + (\mathrm{H}_{22} - \mathrm{H}_{33})(\mathrm{H}'_{11} - \mathrm{H}'_{33}))\,\hat{I}_{80}. \tag{93}$$

The axisymmetric case is recovered by letting $\mathrm{H}_{11}{=}1{-}3\kappa$, $\mathrm{H}_{22}{=}\mathrm{H}_{33}{=}\kappa$ and $\mathrm{H}'_{22}{=}1{-}3\kappa'$, $\mathrm{H}'_{11}{=}\mathrm{H}'_{33}{=}\kappa'$, in which case (85)–(87), (88)–(90), and (91)–(93) become, respectively, (57), the factor in parenthesis in (58), and (59).

C Appendix C. Analytical expressions for stress components in shear and biaxial tests

Shear deformation Consider orthonormal basis $\{\mathbf{f}_0, \mathbf{s}_0, \mathbf{n}_0\}$. Let $\mathbf{M} = \mathbf{f}_0$, $\mathbf{M}' = \mathbf{s}_0$, $\mathbf{H} = \mathrm{diag}(\mathrm{H}_{11}, \mathrm{H}_{22}, \mathrm{H}_{33})$, $\mathbf{H}' = \mathrm{diag}(\mathrm{H}'_{11}, \mathrm{H}'_{22}, \mathrm{H}'_{33})$. For a simple shear deformation corresponding to the deformation gradient $\mathbf{F}_{\mathrm{fs}} = \mathbf{1} + \gamma\mathbf{s}_0\otimes\mathbf{f}_0$, we have

$$\mathbf{C} = \mathbf{1} + \gamma^2\mathbf{f}_0\otimes\mathbf{f}_0 + 2\gamma[\mathbf{f}_0\otimes\mathbf{s}_0]_{\mathrm{sym}}, \quad \mathbf{C}^2 = \mathbf{1} + \left(3\gamma^2 + \gamma^4\right)\mathbf{f}_0\otimes\mathbf{f}_0 + \gamma^2\mathbf{s}_0\otimes\mathbf{s}_0 + \left(4\gamma + 2\gamma^3\right)[\mathbf{f}_0\otimes\mathbf{s}_0]_{\mathrm{sym}}, \tag{94}$$
$$\mathbf{b} = \mathbf{1} + \gamma^2\mathbf{s}_0\otimes\mathbf{s}_0 + 2\gamma[\mathbf{f}_0\otimes\mathbf{s}_0]_{\mathrm{sym}}, \quad \mathbf{b}^2 = \mathbf{1} + \gamma^2\mathbf{f}_0\otimes\mathbf{f}_0 + \left(3\gamma^2 + \gamma^4\right)\mathbf{s}_0\otimes\mathbf{s}_0 + \left(4\gamma + 2\gamma^3\right)[\mathbf{f}_0\otimes\mathbf{s}_0]_{\mathrm{sym}}, \tag{95}$$
$$\mathbf{C}^{-1} = \mathbf{1} + \gamma^2\mathbf{s}_0\otimes\mathbf{s}_0 - 2\gamma[\mathbf{f}_0\otimes\mathbf{s}_0]_{\mathrm{sym}}, \qquad \mathbf{b}^{-1} = \mathbf{1} + \gamma^2\mathbf{f}_0\otimes\mathbf{f}_0 - 2\gamma[\mathbf{f}_0\otimes\mathbf{s}_0]_{\mathrm{sym}}, \tag{96}$$
$$I_1 = I_2 = 3 + \gamma^2, \quad I_4 = I_7 = 1 + \gamma^2, \quad I_5 = 1 + 3\gamma^2 + \gamma^4, \quad I_6 = 1, \quad I_8 = I_{80} = \gamma. \tag{97}$$
$$I^*_4 = (1 + \gamma^2)\mathrm{H}_{11} + \mathrm{H}_{22} + \mathrm{H}_{33}, \quad I^*_6 = (1 + \gamma^2)\mathrm{H}'_{11} + \mathrm{H}'_{22} + \mathrm{H}'_{33}, \tag{98}$$
$$I^*_5 = (1 + 3\gamma^2 + \gamma^4)\mathrm{H}_{11} + (1 + \gamma^2)\mathrm{H}_{22} + \mathrm{H}_{33}, \quad I^*_7 = (1 + 3\gamma^2 + \gamma^4)\mathrm{H}'_{11} + (1 + \gamma^2)\mathrm{H}'_{22} + \mathrm{H}'_{33}, \tag{99}$$
$$\hat{I}^*_8 = (1 + \gamma^2)^2\mathrm{H}_{11}\mathrm{H}'_{11} + \mathrm{H}_{22}\mathrm{H}'_{22} + \mathrm{H}_{33}\mathrm{H}'_{33} + (\mathrm{H}_{11}\mathrm{H}'_{22} + \mathrm{H}_{22}\mathrm{H}'_{11})\,\gamma^2, \tag{100}$$
$$\hat{I}^*_{80} = \gamma^4\mathrm{H}_{11}\mathrm{H}'_{11} + \gamma^2\,(\mathrm{H}_{11}\mathrm{H}'_{22} + \mathrm{H}_{22}\mathrm{H}'_{11})\,, \tag{101}$$

$$
\begin{aligned}
&\mathbf{h}=\mathbf{F}\mathbf{H}\mathbf{F}^T=\mathbf{H}+2\gamma \mathrm{H}_{11}[\mathbf{f}_0\otimes\mathbf{s}_0]_{\mathrm{sym}}+\gamma^2\mathrm{H}_{11}\mathbf{s}_0\otimes\mathbf{s}_0, && (102)\\
&[\mathbf{CH}]_{\mathrm{sym}}=\mathbf{H}+\gamma(\mathrm{H}_{11}+\mathrm{H}_{22})[\mathbf{f}_0\otimes\mathbf{s}_0]_{\mathrm{sym}}+\gamma^2\mathrm{H}_{11}\mathbf{f}_0\otimes\mathbf{f}_0, && (103)\\
&[\mathbf{bh}]_{\mathrm{sym}}=\mathbf{H}+\gamma^2\mathrm{H}_{11}\mathbf{f}_0\otimes\mathbf{f}_0+\left((2\gamma^2+\gamma^4)\mathrm{H}_{11}+\gamma^2\mathrm{H}_{22}\right)\mathbf{s}_0\otimes\mathbf{s}_0+\left((3\gamma+2\gamma^3)\mathrm{H}_{11}+\gamma\mathrm{H}_{22}\right)[\mathbf{f}_0\otimes\mathbf{s}_0]_{\mathrm{sym}}, && (104)\\
&[\mathbf{H}\,(\mathbf{C}-\mathbf{1})\,\mathbf{H}']_{\mathrm{sym}}=\gamma^2\mathrm{H}_{11}\mathrm{H}'_{11}\mathbf{f}_0\otimes\mathbf{f}_0+\gamma(\mathrm{H}_{11}\mathrm{H}'_{22}+\mathrm{H}_{22}\mathrm{H}'_{11})[\mathbf{f}_0\otimes\mathbf{s}_0]_{\mathrm{sym}}, && (105)\\
&\left[\mathbf{h}\left(\mathbf{1}-\mathbf{b}^{-1}\right)\mathbf{h}'\right]_{\mathrm{sym}}=\gamma^2\mathrm{H}_{11}\mathrm{H}'_{11}\mathbf{f}_0\otimes\mathbf{f}_0+\left(\gamma^2(\mathrm{H}_{11}\mathrm{H}'_{22}+\mathrm{H}_{22}\mathrm{H}'_{11})+\gamma^4\mathrm{H}_{11}\mathrm{H}'_{11}\right)\mathbf{s}_0\otimes\mathbf{s}_0 && (106)\\
&\qquad+\left(\gamma(\mathrm{H}_{11}\mathrm{H}'_{22}+\mathrm{H}_{22}\mathrm{H}'_{11})+2\gamma^3\mathrm{H}_{11}\mathrm{H}'_{11}\right)[\mathbf{f}_0\otimes\mathbf{s}_0]_{\mathrm{sym}}, && (107)
\end{aligned}
$$

where expressions for $\mathbf{h}'$, $[\mathbf{CH}']_{\mathrm{sym}}$, and $[\mathbf{bh}']_{\mathrm{sym}}$ are analogous to $\mathbf{h}$, $[\mathbf{CH}]_{\mathrm{sym}}$, and $[\mathbf{bh}]_{\mathrm{sym}}$. Using the above, we can specialise the Cauchy stress tensor (26)–(27), whose only non-zero entries are

$$
\begin{aligned}
\sigma_{\mathrm{ff}}&=-p+2\Psi_1+4\Psi_2+2\mathrm{H}_{11}\Psi_4+4\mathrm{H}_{11}(1+\gamma^2)\Psi_5+2\mathrm{H}'_{11}\Psi_6+4\mathrm{H}'_{11}(1+\gamma^2)\Psi_7+4\mathrm{H}_{11}\mathrm{H}'_{11}\gamma^2\Psi_{\hat{8}0}, && (108)\\
\sigma_{\mathrm{ss}}&=-p+2(1+\gamma^2)\Psi_1+2(2+\gamma^2)\Psi_2+2(\gamma^2\mathrm{H}_{11}+\mathrm{H}_{22})\Psi_4+\left((2\gamma^2+\gamma^4)\mathrm{H}_{11}+(1+\gamma^2)\mathrm{H}_{22}\right)\Psi_5\\
&\quad+2(\gamma^2\mathrm{H}'_{11}+\mathrm{H}'_{22})\Psi_6+\left((2\gamma^2+\gamma^4)\mathrm{H}'_{11}+(1+\gamma^2)\mathrm{H}'_{22}\right)\Psi_7+4\gamma^2\left(\mathrm{H}_{11}\mathrm{H}'_{22}+\mathrm{H}_{22}\mathrm{H}'_{11}+\gamma^2\mathrm{H}_{11}\mathrm{H}'_{11}\right)\Psi_{\hat{8}0}, && (109)\\
\sigma_{\mathrm{nn}}&=-p+2\Psi_1+(4+2\gamma^2)\Psi_2+2\mathrm{H}_{33}\Psi_4+4\mathrm{H}_{33}\Psi_5+2\mathrm{H}'_{33}\Psi_6+4\mathrm{H}'_{33}\Psi_7,\\
\sigma_{\mathrm{fs}}&=2\gamma\Psi_1+2\gamma\Psi_2+2\gamma\mathrm{H}_{11}\Psi_4+2\gamma((3+2\gamma^2)\mathrm{H}_{11}+\mathrm{H}_{22})\Psi_5+2\gamma\mathrm{H}'_{11}\Psi_6+2\gamma((3+2\gamma^2)\mathrm{H}'_{11}+\mathrm{H}'_{22})\Psi_7\\
&\quad+2\gamma\left(\mathrm{H}_{11}\mathrm{H}'_{22}+\mathrm{H}_{22}\mathrm{H}'_{11}+2\gamma^2\mathrm{H}_{11}\mathrm{H}'_{11}\right)\Psi_{\hat{8}0}, && (110)
\end{aligned}
$$

where $\sigma_{\mathrm{fs}}(\gamma)$ is the function of interest. Shear stresses corresponding to other shear modes are obtained in a similar way,

$$
\begin{aligned}
\sigma_{\mathrm{fn}}&=2\gamma\Psi_1+2\gamma\Psi_2+2\gamma\mathrm{H}_{11}\Psi_4+2\gamma((3+2\gamma^2)\mathrm{H}_{11}+\mathrm{H}_{33})\Psi_5+2\gamma\mathrm{H}'_{11}\Psi_6+2\gamma((3+2\gamma^2)\mathrm{H}'_{11}+\mathrm{H}'_{33})\Psi_7\\
&\quad+2\gamma\left(\mathrm{H}_{11}\mathrm{H}'_{33}+\mathrm{H}_{33}\mathrm{H}'_{11}+2\gamma^2\mathrm{H}_{11}\mathrm{H}'_{11}\right)\Psi_{\hat{8}0}, && (111)
\end{aligned}
$$

$$
\begin{aligned}
\sigma_{\mathrm{sf}}&=2\gamma\Psi_1+2\gamma\Psi_2+2\gamma\mathrm{H}_{22}\Psi_4+2\gamma((3+2\gamma^2)\mathrm{H}_{22}+\mathrm{H}_{11})\Psi_5+2\gamma\mathrm{H}'_{22}\Psi_6+2\gamma((3+2\gamma^2)\mathrm{H}'_{22}+\mathrm{H}'_{11})\Psi_7\\
&\quad+2\gamma\left(\mathrm{H}_{11}\mathrm{H}'_{22}+\mathrm{H}_{22}\mathrm{H}'_{11}+2\gamma^2\mathrm{H}_{22}\mathrm{H}'_{22}\right)\Psi_{\hat{8}0}, && (112)
\end{aligned}
$$

$$
\begin{aligned}
\sigma_{\mathrm{sn}}&=2\gamma\Psi_1+2\gamma\Psi_2+2\gamma\mathrm{H}_{22}\Psi_4+2\gamma((3+2\gamma^2)\mathrm{H}_{22}+\mathrm{H}_{33})\Psi_5+2\gamma\mathrm{H}'_{22}\Psi_6+2\gamma((3+2\gamma^2)\mathrm{H}'_{22}+\mathrm{H}'_{33})\Psi_7\\
&\quad+2\gamma\left(\mathrm{H}_{33}\mathrm{H}'_{22}+\mathrm{H}_{22}\mathrm{H}'_{33}+2\gamma^2\mathrm{H}_{22}\mathrm{H}'_{22}\right)\Psi_{\hat{8}0}, && (113)
\end{aligned}
$$

$$
\begin{aligned}
\sigma_{\mathrm{nf}}&=2\gamma\Psi_1+2\gamma\Psi_2+2\gamma\mathrm{H}_{33}\Psi_4+2\gamma((3+2\gamma^2)\mathrm{H}_{33}+\mathrm{H}_{11})\Psi_5+2\gamma\mathrm{H}'_{33}\Psi_6+2\gamma((3+2\gamma^2)\mathrm{H}'_{33}+\mathrm{H}'_{11})\Psi_7\\
&\quad+2\gamma\left(\mathrm{H}_{11}\mathrm{H}'_{33}+\mathrm{H}_{33}\mathrm{H}'_{11}+2\gamma^2\mathrm{H}_{33}\mathrm{H}'_{33}\right)\Psi_{\hat{8}0}, && (114)
\end{aligned}
$$

$$
\begin{aligned}
\sigma_{\mathrm{ns}}&=2\gamma\Psi_1+2\gamma\Psi_2+2\gamma\mathrm{H}_{33}\Psi_4+2\gamma((3+2\gamma^2)\mathrm{H}_{33}+\mathrm{H}_{22})\Psi_5+2\gamma\mathrm{H}'_{33}\Psi_6+2\gamma((3+2\gamma^2)\mathrm{H}'_{33}+\mathrm{H}'_{22})\Psi_7\\
&\quad+2\gamma\left(\mathrm{H}_{33}\mathrm{H}'_{22}+\mathrm{H}_{22}\mathrm{H}'_{33}+2\gamma^2\mathrm{H}_{33}\mathrm{H}'_{33}\right)\Psi_{\hat{8}0}. && (115)
\end{aligned}
$$

The form of the expressions (110)–(115) is the same, up to a permutation of indices in GSTs' components (e.g., σ_{ns} is obtained from σ_{fs} by replacing $(\mathrm{f},\mathrm{s},\mathrm{n})\rightarrow(\mathrm{n},\mathrm{s},\mathrm{f})$). Note that Ψ_i in (110)–(115) implicitly depend on invariants, which may be different functions in different deformation modes, that is, Ψ_4 in (110) is not the same as Ψ_4 in (115).

Now we write $\sigma_{\mathrm{fs}},\ldots,\sigma_{\mathrm{ns}}$ for the special case of Holzapfel–Ogden model with axisymmetric fibre dispersion (69),

$$
\begin{aligned}
\sigma_{\mathrm{fs}}&=a\gamma\exp\left[b\gamma^2\right]+a_{\mathrm{f}}\gamma^3(1-2\kappa)^2\exp\left[b_{\mathrm{f}}\gamma^4(1-2\kappa)^2\right]+a_{\mathrm{s}}\gamma^3\kappa'^2\exp\left[b_{\mathrm{s}}\gamma^4\kappa'^2\right]\\
&\quad+a_{\mathrm{fs}}\gamma\left(\left(1-2\kappa'-2\kappa+5\kappa\kappa'\right)\right)+\gamma^2(2-4\kappa)\kappa'\right)\exp\left[b_{\mathrm{bf}}\gamma^2\left(\left(1-2\kappa-2\kappa'+5\kappa\kappa'\right)+\gamma^2\kappa'(1-2\kappa)\right)\right], && (116)
\end{aligned}
$$

$$
\begin{aligned}
\sigma_{\mathrm{fn}} &= a\gamma \exp\left[b\gamma^2\right] + a_{\mathrm{f}}\gamma^3(1-2\kappa)^2 \exp\left[b_{\mathrm{f}}\gamma^4(1-2\kappa)^2\right] + a_{\mathrm{s}}\gamma^3\kappa'^2 \exp\left[b_{\mathrm{s}}\gamma^4\kappa'^2\right] \\
&\quad + a_{\mathrm{fs}}\gamma\left((\kappa' - \kappa\kappa') + \gamma^2(2-4\kappa)\kappa'\right)\exp\left[b_{\mathrm{bf}}\gamma^2\left(\kappa'(1-\kappa) + \gamma^2\kappa'(1-2\kappa)\right)\right],
\end{aligned} \tag{117}
$$

$$
\begin{aligned}
\sigma_{\mathrm{sf}} &= a\gamma \exp\left[b\gamma^2\right] + a_{\mathrm{f}}\gamma^3\kappa^2 \exp\left[b_{\mathrm{f}}\gamma^4\kappa^2\right] + a_{\mathrm{s}}\gamma^3(1-2\kappa')^2 \exp\left[b_{\mathrm{s}}\gamma^4(1-2\kappa')^2\right] \\
&\quad + a_{\mathrm{fs}}\gamma\left((1-2\kappa'-2\kappa+5\kappa\kappa')) + \gamma^2\kappa(2-4\kappa')\right)\exp\left[b_{\mathrm{bf}}\gamma^2\left((1-2\kappa-2\kappa'+5\kappa\kappa') + \gamma^2\kappa(1-2\kappa')\right)\right],
\end{aligned} \tag{118}
$$

$$
\begin{aligned}
\sigma_{\mathrm{sn}} &= a\gamma \exp\left[b\gamma^2\right] + a_{\mathrm{f}}\gamma^3\kappa^2 \exp\left[b_{\mathrm{f}}\gamma^4\kappa^2\right] + a_{\mathrm{s}}\gamma^3(1-2\kappa')^2 \exp\left[b_{\mathrm{s}}\gamma^4(1-2\kappa')^2\right] \\
&\quad + a_{\mathrm{fs}}\gamma\left((\kappa - \kappa\kappa') + \gamma^2\kappa(2-4\kappa')\right)\exp\left[b_{\mathrm{bf}}\gamma^2\left((\kappa-\kappa\kappa') + \gamma^2\kappa(1-2\kappa')\right)\right],
\end{aligned} \tag{119}
$$

$$
\begin{aligned}
\sigma_{\mathrm{nf}} &= a\gamma \exp\left[b\gamma^2\right] + a_{\mathrm{f}}\gamma^3\kappa^2 \exp\left[b_{\mathrm{f}}\gamma^4\kappa^2\right] + a_{\mathrm{s}}\gamma^3\kappa'^2 \exp\left[b_{\mathrm{s}}\gamma^4\kappa'^2\right] \\
&\quad + a_{\mathrm{fs}}\gamma\left((\kappa' - \kappa\kappa') + 2\gamma^2\kappa\kappa'\right)\exp\left[b_{\mathrm{bf}}\gamma^2\left((\kappa'-\kappa\kappa') + \gamma^2\kappa\kappa'\right)\right],
\end{aligned} \tag{120}
$$

$$
\begin{aligned}
\sigma_{\mathrm{ns}} &= a\gamma \exp\left[b\gamma^2\right] + a_{\mathrm{f}}\gamma^3\kappa^2 \exp\left[b_{\mathrm{f}}\gamma^4\kappa^2\right] + a_{\mathrm{s}}\gamma^3\kappa'^2 \exp\left[b_{\mathrm{s}}\gamma^4\kappa'^2\right] \\
&\quad + a_{\mathrm{fs}}\gamma\left((\kappa - \kappa\kappa') + 2\gamma^2\kappa\kappa'\right)\exp\left[b_{\mathrm{bf}}\gamma^2\left((\kappa-\kappa\kappa') + \gamma^2\kappa\kappa'\right)\right].
\end{aligned} \tag{121}
$$

One can see, for instance, that the difference between $\sigma_{\mathrm{nf}} - \sigma_{\mathrm{ns}}$ vanishes for $\kappa = \kappa'$. It can be expected and is shown in Figure 3b that the difference $|\sigma_{\mathrm{nf}} - \sigma_{\mathrm{ns}}|$ is a monotonous function of $|\kappa - \kappa'|$.

Biaxial stretching With the same assumptions, as for the shear deformation modes, consider $\mathbf{F} = \mathrm{diag}(\lambda_1, \lambda_2, \lambda_3)$, where $\lambda_3 = \lambda_1^{-1}\lambda_2^{-1}$ is assumed satisfy the incompressibility condition. A biaxial stretch protocol is introduced by imposing a relation between λ_1 and λ_2 and the boundary condition $\sigma_{33} = 0$, which is consistent with the deformation being considered. The expressions for the deformation invariants read

$$
I_1 = \lambda_1^2 + \lambda_2^2 + \lambda_1^{-2}\lambda_2^{-2}, \quad I_2 = \lambda_1^{-2} + \lambda_2^{-2} + \lambda_1^2\lambda_2^2, \tag{122}
$$

$$
I_4 = \lambda_1^2, \quad I_5 = \lambda_1^4, \quad I_6 = \lambda_2^2, \quad I_7 = \lambda_2^4, \quad I_8 = I_{80} = 0, \tag{123}
$$

$$
I_4^* = \mathrm{H}_{11}\lambda_1^2 + \mathrm{H}_{22}\lambda_2^2 + \mathrm{H}_{33}\lambda_1^{-2}\lambda_2^{-2}, \quad I_6^* = \mathrm{H}'_{11}\lambda_1^2 + \mathrm{H}'_{22}\lambda_2^2 + \mathrm{H}'_{33}\lambda_1^{-2}\lambda_2^{-2}, \tag{124}
$$

$$
I_5^* = \mathrm{H}_{11}\lambda_1^4 + \mathrm{H}_{22}\lambda_2^4 + \mathrm{H}_{33}\lambda_1^{-4}\lambda_2^{-4}, \quad I_7^* = \mathrm{H}'_{11}\lambda_1^4 + \mathrm{H}'_{22}\lambda_2^4 + \mathrm{H}'_{33}\lambda_1^{-4}\lambda_2^{-4}, \tag{125}
$$

$$
\hat{I}_8^* = \mathrm{H}_{11}\mathrm{H}'_{11}\lambda_1^4 + \mathrm{H}_{22}\mathrm{H}'_{22}\lambda_2^4 + \mathrm{H}_{33}\mathrm{H}'_{33}\lambda_1^{-4}\lambda_2^{-4}, \tag{126}
$$

$$
\hat{I}_{80}^* = \mathrm{H}_{11}\mathrm{H}'_{11}\left(\lambda_1^2 - 1\right)^2 + \mathrm{H}_{22}\mathrm{H}'_{22}\left(\lambda_2^2 - 1\right)^2 + \mathrm{H}_{33}\mathrm{H}'_{33}\left(\lambda_1^{-2}\lambda_2^{-2} - 1\right)^2. \tag{127}
$$

All the tensors involved in (26)–(27) are diagonal in the basis $\{\mathbf{f}_0, \mathbf{s}_0, \mathbf{n}_0\}$, so are the resulting stress tensors. For instance, we have $\mathbf{C} = \mathbf{b} = \mathrm{diag}(\lambda_1^2, \lambda_2^2, \lambda_1^{-2}\lambda_2^{-2})$, $\mathbf{h} = \mathrm{diag}(\mathrm{H}_{11}\lambda_1^2, \mathrm{H}_{22}\lambda_2^2, \mathrm{H}_{33}\lambda_1^{-2}\lambda_2^{-2})$, etc. The non-zero entries of the Cauchy stress tensor are

$$
\begin{aligned}
\sigma_{11} &= -p + 2\lambda_1^2\Psi_1 + 2\left(\frac{1}{\lambda_2^2} + \lambda_1^2\lambda_2^2\right)\Psi_2 + 2\mathrm{H}_{11}\lambda_1^2\Psi_4 + 4\mathrm{H}_{11}\lambda_1^4\Psi_5 + 2\mathrm{H}'_{11}\lambda_1^2\Psi_6 + 4\mathrm{H}'_{11}\lambda_1^4\Psi_7 + 4\mathrm{H}_{11}\mathrm{H}'_{11}\lambda_1^2\left(\lambda_1^2 - 1\right)\Psi_{\hat{8}0}, \\
\sigma_{22} &= -p + 2\lambda_2^2\Psi_1 + 2\left(\frac{1}{\lambda_1^2} + \lambda_1^2\lambda_2^2\right)\Psi_2 + 2\mathrm{H}_{22}\lambda_2^2\Psi_4 + 4\mathrm{H}_{22}\lambda_2^4\Psi_5 + 2\mathrm{H}'_{22}\lambda_2^2\Psi_6 + 4\mathrm{H}'_{22}\lambda_2^4\Psi_7 + 4\mathrm{H}_{22}\mathrm{H}'_{22}\lambda_2^2\left(\lambda_2^2 - 1\right)\Psi_{\hat{8}0}, \\
\sigma_{33} &= -p + \frac{2}{\lambda_1^2\lambda_2^2}\Psi_1 + 2\left(\frac{1}{\lambda_1^2} + \frac{1}{\lambda_2^2}\right)\Psi_2 + 2\mathrm{H}_{33}\frac{1}{\lambda_1^2\lambda_2^2}\Psi_4 + 4\mathrm{H}_{33}\frac{1}{\lambda_1^4\lambda_2^4}\Psi_5 + 2\mathrm{H}'_{33}\frac{1}{\lambda_1^2\lambda_2^2}\Psi_6 + 4\mathrm{H}'_{33}\frac{1}{\lambda_1^4\lambda_2^4}\Psi_7 + 4\mathrm{H}_{33}\mathrm{H}'_{33}\frac{\lambda_1^2\lambda_2^2 - 1}{\lambda_1^4\lambda_2^4}\Psi_{\hat{8}0}.
\end{aligned} \tag{128}
$$

The boundary condition $\sigma_{33} = 0$ defines the incompressibility-associated Lagrange multiplier p. For the special case of the Holzapfel–Ogden model with axisymmetric fibre dispersion (69), we have

$$\sigma_{11} = 2\left(\lambda_1^2 - \frac{1}{\lambda_1^2\lambda_2^2}\right)\Psi_1 + 2\left(\lambda_1^2\lambda_2^2 - \frac{1}{\lambda_1^2}\right)\Psi_2 + 2\left(\mathrm{H}_{11}\lambda_1^2 - \mathrm{H}_{33}\frac{1}{\lambda_1^2\lambda_2^2}\right)\Psi_4 + 4\left(\mathrm{H}_{11}\lambda_1^4 - \mathrm{H}_{33}\frac{1}{\lambda_1^4\lambda_2^4}\right)\Psi_5 \tag{129}$$

$$+ 2\left(\mathrm{H}'_{11}\lambda_1^2 - \mathrm{H}'_{33}\frac{1}{\lambda_1^2\lambda_2^2}\right)\Psi_6 + 4\left(\mathrm{H}'_{11}\lambda_1^4 - \mathrm{H}'_{33}\frac{1}{\lambda_1^4\lambda_2^4}\right)\Psi_7 + 4\left(\mathrm{H}_{11}\mathrm{H}'_{11}\left(\lambda_1^4 - \lambda_1^2\right) - \mathrm{H}_{33}\mathrm{H}'_{33}\left(\frac{1}{\lambda_1^2\lambda_2^2} - \frac{1}{\lambda_1^4\lambda_2^4}\right)\right)\Psi_{\hat{8}0}, \tag{130}$$

$$\sigma_{22} = 2\left(\lambda_2^2 - \frac{1}{\lambda_1^2\lambda_2^2}\right)\Psi_1 + 2\left(\lambda_1^2\lambda_2^2 - \frac{1}{\lambda_2^2}\right)\Psi_2 + 2\left(\mathrm{H}_{22}\lambda_2^2 - \mathrm{H}_{33}\frac{1}{\lambda_1^2\lambda_2^2}\right)\Psi_4 + 4\left(\mathrm{H}_{22}\lambda_2^4 - \mathrm{H}_{33}\frac{1}{\lambda_1^4\lambda_2^4}\right)\Psi_5$$

$$+ 2\left(\mathrm{H}'_{22}\lambda_2^2 - \mathrm{H}'_{33}\frac{1}{\lambda_1^2\lambda_2^2}\right)\Psi_6 + 4\left(\mathrm{H}'_{22}\lambda_2^4 - \mathrm{H}'_{33}\frac{1}{\lambda_1^4\lambda_2^4}\right)\Psi_7 + 4\left(\mathrm{H}_{22}\mathrm{H}'_{22}\left(\lambda_2^4 - \lambda_2^2\right) - \mathrm{H}_{33}\mathrm{H}'_{33}\left(\frac{1}{\lambda_1^2\lambda_2^2} - \frac{1}{\lambda_1^4\lambda_2^4}\right)\right)\Psi_{\hat{8}0},$$

$$\sigma_{11} = a\left(\lambda_1^2 - \frac{1}{\lambda_1^2\lambda_2^2}\right)\exp\left[b\left(\lambda_1^2 + \lambda_2^2 + \frac{1}{\lambda_1^2\lambda_2^2} - 3\right)\right] \tag{131}$$

$$+ a_{\mathrm{f}}\left((1-2\kappa)\lambda_1^2 - \kappa\frac{1}{\lambda_1^2\lambda_2^2}\right)\left((1-2\kappa)\left(\lambda_1^2 - 1\right) + \kappa\left(\lambda_2^2 + \frac{1}{\lambda_1^2\lambda_2^2} - 2\right)\right)\exp\left[b_{\mathrm{f}}\left((1-2\kappa)\left(\lambda_1^2 - 1\right) + \kappa\left(\lambda_2^2 + \frac{1}{\lambda_1^2\lambda_2^2} - 2\right)\right)^2\right] \tag{132}$$

$$+ a_{\mathrm{s}}\kappa'\left(\lambda_1^2 - \frac{1}{\lambda_1^2\lambda_2^2}\right)\left(\kappa'\left(\lambda_1^2 + \frac{1}{\lambda_1^2\lambda_2^2} - 2\right) + \left(1-2\kappa'\right)\lambda_2^2\right)\exp\left[b_{\mathrm{s}}\left(\kappa'\left(\lambda_1^2 + \frac{1}{\lambda_1^2\lambda_2^2} - 2\right) + \left(1-2\kappa'\right)\lambda_2^2\right)^2\right] \tag{133}$$

$$+ 2a_{\mathrm{fs}}\left((1-2\kappa)\kappa'\lambda_1^2\left(\lambda_1^2 - 1\right) + \kappa\kappa'\left(\frac{1}{\lambda_1^2\lambda_2^2} - \frac{1}{\lambda_1^4\lambda_2^4}\right)^2\right)\exp\left[b_{\mathrm{fs}}\left((1-2\kappa)\kappa'\left(\lambda_1^2 - 1\right)^2 + \kappa(1-2\kappa')\left(\lambda_2^2 - 1\right)^2 + \kappa\kappa'\left(\frac{1}{\lambda_1^2\lambda_2^2} - 1\right)^2\right)\right] \tag{134}$$

$$\sigma_{22} = a\left(\lambda_2^2 - \frac{1}{\lambda_1^2\lambda_2^2}\right)\exp\left[b\left(\lambda_1^2 + \lambda_2^2 + \frac{1}{\lambda_1^2\lambda_2^2} - 3\right)\right]$$

$$+ a_{\mathrm{f}}\kappa\left(\lambda_2^2 - \frac{1}{\lambda_1^2\lambda_2^2}\right)\left((1-2\kappa)\left(\lambda_1^2 - 1\right) + \kappa\left(\lambda_2^2 + \frac{1}{\lambda_1^2\lambda_2^2} - 2\right)\right)\exp\left[b_{\mathrm{f}}\left((1-2\kappa)\left(\lambda_1^2 - 1\right) + \kappa\left(\lambda_2^2 + \frac{1}{\lambda_1^2\lambda_2^2} - 2\right)\right)^2\right]$$

$$+ a_{\mathrm{s}}\left(\left(1-2\kappa'\right)\lambda_2^2 - \kappa'\frac{1}{\lambda_1^2\lambda_2^2}\right)\left(\kappa'\left(\lambda_1^2 + \frac{1}{\lambda_1^2\lambda_2^2} - 2\right) + \left(1-2\kappa'\right)\lambda_2^2\right)\exp\left[b_{\mathrm{s}}\left(\kappa'\left(\lambda_1^2 + \frac{1}{\lambda_1^2\lambda_2^2} - 2\right) + \left(1-2\kappa'\right)\lambda_2^2\right)^2\right] \tag{135}$$

$$+ 2a_{\mathrm{fs}}\left(\kappa(1-2\kappa')\lambda_2^2\left(\lambda_2^2 - 1\right) + \kappa\kappa'\left(\frac{1}{\lambda_1^2\lambda_2^2} - \frac{1}{\lambda_1^4\lambda_2^4}\right)^2\right)\exp\left[b_{\mathrm{fs}}\left((1-2\kappa)\kappa'\left(\lambda_1^2 - 1\right)^2 + \kappa(1-2\kappa')\left(\lambda_2^2 - 1\right)^2 + \kappa\kappa'\left(\frac{1}{\lambda_1^2\lambda_2^2} - 1\right)^2\right)\right] \tag{136}$$